

The dual superconformal theory for $L^{p,q,r}$ manifolds

Agostino Butti, Davide Forcella and Alberto Zaffaroni

^a *Dipartimento di Fisica, Università di Milano-Bicocca
P.zza della Scienza, 3; I-20126 Milano, Italy*

Abstract

We present the superconformal gauge theory living on the world-volume of D3 branes probing the toric singularities with horizon the recently discovered Sasaki-Einstein manifolds $L^{p,q,r}$. Various checks of the identification are made by comparing the central charge and the R-charges of the chiral fields with the information that can be extracted from toric geometry. Fractional branes are also introduced and the physics of the associated duality cascade discussed.

agostino.butti@mib.infn.it
davide.forcella@mib.infn.it
alberto.zaffaroni@mib.infn.it

1 Introduction

D3 branes living at conical Calabi-Yau singularities are a good laboratory for the AdS/CFT correspondence since its early days. The world-volume theory on the branes is dual to a type IIB background of the form $AdS_5 \times H$, where H is the horizon manifold [1,2]. The correspondence between conical singularities and superconformal gauge theories has also given information on non-conformal ones. One of the few known examples of regular backgrounds dual to confining gauge theories, the Klebanov-Strassler solution [3], is indeed obtained by introducing fractional branes at a conifold singularity. In the conformal case, supersymmetry requires that H is a Sasaki-Einstein metric. Until few months ago, the only known Sasaki-Einstein metrics were the round sphere S^5 and $T^{1,1}$, the horizon of the conifold. Recently, an infinite class of new regular Sasaki-Einstein metrics with $SU(2) \times U(1) \times U(1)$ isometry was constructed [4]. These manifolds are labeled by two integers \bar{p} and \bar{q} and have been named $Y^{\bar{p},\bar{q}}$. With the determination of the corresponding dual gauge theory [5], new checks of the AdS/CFT correspondence were possible [5–8]. As well known, the central charge of the CFT and the dimension of some operators can be compared with the volumes of H and of some of its submanifolds. In particular, the a-maximization technique [9] now allows for a detailed computation of the relevant quantum field theory quantities. Needless to say, the agreement of the two computations is perfect.

More recently, a generalization of the $Y^{\bar{p},\bar{q}}$ manifolds with smaller isometry $U(1)^3$ and depending on three integers p, q, r has been constructed [10,11]. When p, q and r satisfy some conditions, these Sasaki-Einstein manifolds, named $L^{p,q,r}$, are smooth. In this paper, we will construct the dual superconformal gauge theory, using a powerful method developed in [12]. The precise correspondence between conical Calabi-Yau singularities and superconformal gauge theories is still unknown. However, a remarkable progress has been recently made for the class of Gorenstein toric singularities. The brane tiling (dimers) construction [12], an ingenious generalization of the Brane Boxes [13,14], introduces a direct relation between an Hanany-Witten realization [15] for gauge theory and the toric diagram. In particular, from the quiver associated with a superconformal gauge theory one can determine the dual brane tiling configuration, a dimer lattice. It is then possible to associate a toric diagram with each of these lattices, identifying the dual Calabi-Yau. The inverse process (to associate a gauge theory with a given singularity) is more difficult. Hopefully, in the long period, the dimers technology will allow to define a one-to-one correspondence between CFTs and toric singularities. For the moment, we will determine the superconformal gauge theory by using some analogy with the $Y^{\bar{p},\bar{q}}$ case.

To implement the dimer technology, we need the toric description of the cone over the $L^{p,q,r}$ manifolds. The construction of the toric diagram for all integers p, q, r and the toric description of the Calabi-Yau is described in the first part of this paper using results given in [10,11]. We will also present explicit formulae for the volume of $L^{p,q,r}$ and the volumes of special submanifolds. With the knowledge of the toric diagram, we can engineer a dimer configuration that is general enough to contain all the infinite theories with diagram associated with the numbers p, q, r . We are helped

by the fact that the toric diagram has only four external vertices. In the second part of the paper, we discuss the dual gauge theory. We compute the central charge and the dimensions of dibaryons using the a-maximization technique [9] and we compare these results with the AdS/CFT predictions based on volumes. We find a complete agreement.

Even if expected, the agreement always contains a little bit of magic. In particular, we have two different algebraic procedures for computing the R-symmetry charges of the fields and the volumes. The first is based on the maximization of the central charge. The second one can be efficiently encoded in a geometrical minimization procedure for determining the Reeb vector discovered in [16]. The two procedures deal with different test quantities (the R-charges on one side and the components of the Reeb vector on the other) and with different functions to be extremized. It is remarkable that the two methods give exactly equivalent results. In the case of $L^{p,q,r}$ we are not able to analytically solve the extremization problems. Fortunately, the two procedures can be easily automatized in Mathematica. The numerical coincidence of the results for all p, q, r is indeed impressive.

Notice that the agreement of results in the gauge theory and the supergravity side can be regarded not only as another non-trivial check of the AdS/CFT correspondence, but also as a check of the brane tiling construction [12]. The latter is indeed still at the level of a conjecture. We are quite confident that the conjecture will become soon an established result and will lead to an important improvement of our knowledge in the field.

We also discuss the inclusion of fractional branes. As usual this leads to a duality cascade. Unfortunately, as in the $Y^{\bar{p},\bar{q}}$ case, it is most plausible that the theories associated with smooth $L^{p,q,r}$ have no supersymmetric vacuum. We briefly discuss the arguments leading to these conclusions [17–20].

The paper is organized as follows. In Section 2 we review the formulae for the metric of $L^{p,q,r}$. Section 3 describes the toric geometry of the cones over $L^{p,q,r}$ determining the toric diagram. We also discuss the regularity of the metric for all values of p, q, r using toric geometry. We set up a minimization problem for the determination of the Reeb vector following the results in [16] and we give closed expressions for the volume of the submanifolds associated with the edges of the toric fan. In Section 4 we discuss the tiling. In Section 5 we describe the dual gauge theory and perform the a-maximization. In Section 6 we discuss the inclusion of fractional branes in the game and the related duality cascade. Finally, in the Appendix we give details on the brane construction and provide specific examples.

While finishing this work, a paper with partial overlap appeared [21]. It also presents the central charge and the R-charges of fields. Similar results have been obtained also in [22].

2 The $L^{p,q,r}$ spaces

Recently a new infinite class of five-dimensional Sasaki-Einstein spaces was discovered [10, 11]. They were denoted $L^{p,q,r}$. In this Section, we briefly review the geometry

of these spaces. Elaborating on [10, 11], we give explicit formulae for the metric of these spaces and collect expressions that can be useful for the evaluation of volumes.

Our starting point is a set of D3-branes probing a CY conical singularity [1]. The geometry of the transverse space is a cone with $L^{p,q,r}$ base

$$ds_{\text{CY}}^2 = dr^2 + r^2 ds_{(L^{p,q,r})}^2 \quad (2.1)$$

The smooth $L^{p,q,r}$ spaces are characterized by three coprime positive integers p, q, r with $0 < p \leq q, 0 < r < p + q$. The metrics have $U(1) \times U(1) \times U(1)$ isometry enlarging to $SU(2) \times U(1) \times U(1)$ in the special case $p + q = 2r$, which reduces to the previously-known spaces $Y^{\bar{p},\bar{q}} = L^{\bar{p}-\bar{q},\bar{p}+\bar{q},\bar{p}}$ [4]. The topology of these spaces is $S^3 \times S^2$.

For Sasaki-Einstein spaces one can write the local form of the metric as follows:

$$ds_{(L^{p,q,r})}^2 = (d\tau + \sigma)^2 + ds_4^2 \quad (2.2)$$

In the case of the spaces $L^{p,q,r}$

$$\begin{aligned} ds_4^2 &= \frac{\rho^2 dx^2}{4\Delta_x} + \frac{\rho^2 d\theta^2}{\Delta_\theta} + \frac{\Delta_x}{\rho^2} \left(\frac{\sin^2 \theta}{\alpha} d\phi + \frac{\cos^2 \theta}{\beta} d\psi \right)^2 \\ &+ \frac{\Delta_\theta \sin^2 \theta \cos^2 \theta}{\rho^2} \left(\frac{\alpha - x}{\alpha} d\phi - \frac{\beta - x}{\beta} d\psi \right)^2 \end{aligned} \quad (2.3)$$

where

$$\begin{aligned} \sigma &= \frac{(\alpha - x) \sin^2 \theta}{\alpha} d\phi + \frac{(\beta - x) \cos^2 \theta}{\beta} d\psi \\ \Delta_x &= x(\alpha - x)(\beta - x) - \mu \\ \Delta_\theta &= \alpha \cos^2 \theta + \beta \sin^2 \theta \\ \rho^2 &= \Delta_\theta - x \end{aligned} \quad (2.4)$$

We can set one of the parameters α, β, μ to any non-zero constant by rescaling the other two and x . Hence the metrics depend on two non-trivial parameters, which we will take to be β and μ .

The metrics are in general of cohomogeneity 2, with toric principal orbits $U(1) \times U(1) \times U(1)$. In order to obtain metrics on complete non-singular manifolds we have to take the following range of variables: $0 < \theta < \pi/2, x_1 < x < x_2$, where x_1 and x_2 are the two lowest roots of $\Delta_x = 0$. The ranges of the coordinates ϕ, ψ, τ as well as the toric T^3 action are described in the next Section. In this range there are four degeneration surfaces respectively at $\theta = 0, \theta = \pi/2, x = x_1, x = x_2$ where, in order, the normalized four Killing vectors vanish:

$$\frac{\partial}{\partial \phi}, \quad \frac{\partial}{\partial \psi}, \quad l_i = a_i \frac{\partial}{\partial \phi} + b_i \frac{\partial}{\partial \psi} + c_i \frac{\partial}{\partial \tau} \quad (2.5)$$

where $i = 1, 2$ and

$$a_i = \frac{\alpha c_i}{x_i - \alpha}$$

$$\begin{aligned}
b_i &= \frac{\beta c_i}{x_i - \beta} \\
c_i &= \frac{(\alpha - x_i)(\beta - x_i)}{2(\alpha + \beta)x_i - \alpha\beta - 3x_i^2}
\end{aligned} \tag{2.6}$$

Notice that these quantities satisfy the equation

$$1 + a_i + b_i + 3c_i = 0 \tag{2.7}$$

To obtain a non singular manifold, we have to impose a linear relation among the Killing vectors

$$p l_1 + q l_2 + r \frac{\partial}{\partial \phi} + s \frac{\partial}{\partial \psi} = 0 \tag{2.8}$$

with (p, q, r, s) four coprime integers with

$$p + q = r + s \tag{2.9}$$

Notice that all triples chosen from (p, q, r, s) also are coprime. In order to have smooth geometry in 5-d the parameters need to obey $\alpha, \beta \geq x_2$ with $x_3 \geq x_2 \geq x_1 \geq 0$, which imply $q \geq p > 0$ and $p + q > r > 0$.

If we set $p + q = 2r \Rightarrow r = s \Rightarrow \alpha = \beta$ it easy to see that the $L^{p,q,r}$ spaces reduce to the $Y^{\bar{p},\bar{q}}$ spaces with the relations:

$$\bar{p} - \bar{q} = p, \quad \bar{p} + \bar{q} = q, \quad \bar{p} = r \tag{2.10}$$

For reader convenience we exhibit the transformation laws that convert the metric to the one commonly used for the $Y^{\bar{p},\bar{q}}$ spaces:

$$\bar{\psi}' = 3\tau + \psi + \phi, \quad \bar{\phi} = \phi - \psi, \quad \bar{\beta} = -\phi - \psi, \quad \bar{\theta} = 2\theta, \quad \bar{y} = \frac{3x - \alpha}{2\alpha} \tag{2.11}$$

The $L^{p,q,r}$ metric indeed reduces to

$$\begin{aligned}
ds_{(Y^{\bar{p},\bar{q}})}^2 &= \frac{1 - \bar{y}}{6} (d\bar{\theta}^2 + \sin^2 \bar{\theta} d\bar{\phi}^2) + \frac{d\bar{y}^2}{w(\bar{y})q(\bar{y})} + \frac{1}{36} w(\bar{y})q(\bar{y}) (d\bar{\beta} + \cos \bar{\theta} d\bar{\phi})^2 \\
&+ \frac{d\bar{\psi}'}{3} + \frac{1}{3} (-\cos \bar{\theta} d\bar{\phi} + \bar{y} (d\bar{\beta} + \cos \bar{\theta} d\bar{\phi}))^2
\end{aligned} \tag{2.12}$$

that coincides with the $Y^{\bar{p},\bar{q}}$ metric with

$$\begin{aligned}
w(\bar{y}) &= \frac{2(a - \bar{y}^2)}{1 - \bar{y}} \\
q(\bar{y}) &= \frac{a - 3\bar{y}^2 + 2\bar{y}^3}{a - \bar{y}^2}
\end{aligned} \tag{2.13}$$

and a related to μ by

$$\mu = \frac{4}{27} (1 - a) \alpha^3 \tag{2.14}$$

We can find expressions for x_1, x_2, α, β , in terms of p, q, r, s . Using the equations (2.7, 2.9) and

$$\begin{aligned} pc_1 + qc_2 &= 0 \\ pa_1 + qa_2 + r &= 0 \end{aligned} \quad (2.15)$$

we obtain ¹

$$\begin{aligned} x_1 &= \frac{-rs\alpha^2 + p(s-r)\alpha\beta + sr\beta^2 + (\alpha-\beta)\sqrt{\delta}}{(p-3r)s\alpha + (3s-p)r\beta} \\ x_2 &= \frac{-rs\alpha^2 + q(s-r)\alpha\beta + sr\beta^2 + (\beta-\alpha)\sqrt{\delta}}{(q-3r)s\alpha + (3s-q)r\beta} \end{aligned} \quad (2.16)$$

with

$$\delta = sr(r(q-r)(\alpha^2 - \alpha\beta + \beta^2) + p(r\alpha^2 - (q+r)\alpha\beta + r\beta^2))$$

To find α, β we use the relations $\Delta_{x_1} = \Delta_{x_2} = 0$. By eliminating μ from the first relation we obtain

$$x_1(\alpha - x_1)(\beta - x_1) = x_2(\alpha - x_2)(\beta - x_2) \quad (2.17)$$

and using now equation (2.16) we find the quartic equation

$$\begin{aligned} s^3r\alpha^4 - s^2((q-3r)r + p(p+r))\alpha^3\beta + 2sr(pq - 2(p+q)r + 2r^2)\alpha^2\beta^2 \\ + r^2(2p^2 + 3pq + 2q^2 - 5(p+q)r + 3r^2)\alpha\beta^3 + sr^3\beta^4 = 0 \end{aligned} \quad (2.18)$$

This can be solved to give a long expression for β/α . If we use β, μ as free parameters in the metric (2.2) we can set $\alpha = 1$ and so we have the expressions for $x_1, x_2, \alpha, \beta, \mu$ in function of p, q, r, s . We must verify that the solution of equation (2.18) gives rise to positive definite metrics. This implies $q \geq p$ [10]. Using the metric (2.2) it is easy to find the volume of the $L^{p,q,r}$ spaces

$$V = \frac{\pi^3 |c_1| (x_2 - x_1)(\alpha + \beta - x_1 - x_2)}{\alpha\beta q} \quad (2.19)$$

Each variable in (2.19) is known as a function of p, q, r . Therefore, if we like, we can write a (very long) closed equation for the volume in function of p, q, r .

3 The toric diagram for $L^{p,q,r}$

In this Section we build the toric diagram for the CY singularities with horizon $L^{p,q,r}$. The impatient reader can find all the relevant information about the toric diagram in Figure 1. We also compute the volumes of special submanifolds of $L^{p,q,r}$, using a method developed in [16]. These results will be later compared with those of a-maximization. We refer to [23] for a review of all the necessary notions of toric geometry used in this Section.

¹These equations are strictly valid in the case $r \neq s$.

3.1 Building the toric diagram

In the previous Section we reviewed the local form of the metric of the Calabi-Yau cones over the Sasaki-Einstein spaces $L^{p,q,r}$; the toric action $U(1)^3$ on such cones is locally given by the vectors fields: $\frac{\partial}{\partial\phi}, \frac{\partial}{\partial\psi}, \frac{\partial}{\partial\tau}$.

As reviewed in [23], on (six dimensional) symplectic toric cones M we can define a moment map $\mu: M \rightarrow R^3$ whose image is a three dimensional strictly convex rational polyhedral cone \mathcal{C} (the dual fan, in the language of toric geometry [24]). Moreover the original CY cone is reconstructed as a T^3 fibration over the polyhedral cone, with one or two cycles of the T^3 degenerating over faces or edges respectively of the dual fan. In our case, $L^{p,q,r}$, we know that the image of the momentum map is a polyhedral cone with four faces, since there are only four subvarieties with a degenerating Killing vector field [10]. Such divisors are the submanifolds at $\theta = 0$, $\theta = \pi/2$, $x = x_1$, $x = x_2$, with degenerating vectors given respectively by $\frac{\partial}{\partial\phi}, \frac{\partial}{\partial\psi}, l_1, l_2$ in formula (2.5). With the normalizations of the previous Section, the orbits of these vector fields must be closed with period 2π in order to avoid conical singularities when one approaches the faces of the polyhedral cone [10].

The T^3 fibered over the polyhedral cone is described locally by the coordinates (ϕ, ψ, τ) , but we have not yet given a global description of the T^3 action and of the closed orbits. For example, we expect that in general the orbits of the Reeb vector $\frac{\partial}{\partial\tau}$ will not be closed except for the regular (or quasi-regular) case [23]. The toric action can be described giving three identifications in the space (ϕ, ψ, τ) along three independent directions, or equivalently giving a basis of Killing vectors e_1, e_2, e_3 that describe an effectively acting T^3 [23]. e_1, e_2, e_3 will be a linear combination of $\frac{\partial}{\partial\phi}, \frac{\partial}{\partial\psi}, \frac{\partial}{\partial\tau}$ and we understand that they are normalized such that their orbit is closed with period 2π . Of course any $SL(3, Z)$ combination of the e_i will also be a good basis; as usual, the toric diagram is only defined up to $SL(3, Z)$ transformations [24]. Notice that we are building the T^3 action so as to obtain a regular CY cone at $r \neq 0$.

The degenerating vectors can be written as linear combinations of the e_i :

$$\begin{pmatrix} l_1 \\ l_2 \\ \frac{\partial}{\partial\phi} \\ \frac{\partial}{\partial\psi} \end{pmatrix} = \begin{pmatrix} A_{11} & A_{12} & A_{13} \\ A_{21} & A_{22} & A_{23} \\ A_{31} & A_{32} & A_{33} \\ A_{41} & A_{42} & A_{43} \end{pmatrix} \begin{pmatrix} e_1 \\ e_2 \\ e_3 \end{pmatrix} \quad (3.1)$$

Now notice that the four vectors orthogonal to the faces of the polyhedral cone are just the killing vectors that vanish on such faces [23]; the coordinates of such vectors in the basis e_i are just the integers vectors in R^3 that describe the toric diagram (fan). Therefore in our notation the fan is simply generated by the four lines of the matrix A_{ij} . To avoid additional singularities the coefficients A_{ij} must be integers and each triple A_{ij} with fixed i must be coprime, so that the fan is generated by primitive vectors. Up to now there is only a possible ambiguity in the choice of signs for the vectors of the fan; conventionally they are all inward pointing. We now use the fact that for a CY cone we can perform an $SL(3, Z)$ transformation to set the first coordinate of the vectors of the toric diagram equal to one, that is $A_{1,j} = \pm 1$.

But then the requirement (2.8)

$$pl_1 + ql_2 + r \frac{\partial}{\partial \phi} + s \frac{\partial}{\partial \psi} = 0 \quad (3.2)$$

and the equality $p+q = r+s$ gives us the choice $A_{11} = A_{12} = -1$, and $A_{13} = A_{14} = 1$. At this point we can perform another $SL(3, Z)$ transformation to set the remaining two components of, say, l_1 to $(0, 0)$. Our matrix becomes:

$$\begin{pmatrix} -l_1 \\ -l_2 \\ \frac{\partial}{\partial \phi} \\ \frac{\partial}{\partial \psi} \end{pmatrix} = \begin{pmatrix} 1 & 0 & 0 \\ 1 & P & Q \\ 1 & R & S \\ 1 & F & G \end{pmatrix} \begin{pmatrix} e_1 \\ e_2 \\ e_3 \end{pmatrix} \quad (3.3)$$

In the physics literature, it is common to give, instead of the three-dimensional vectors defining the fan, the toric diagram consisting in the projection of the vectors on the plane where they all live. In this case, the toric diagram is given by ignoring the first coordinate and consists of the points: $(0, 0)$, (R, S) , (P, Q) , (F, G) .

Let us study the smoothness of the CY cone. Consider the face $x = x_1$ where l_1 degenerates; the T^3 fibration over this face reduces to a T^2 fibration and the corresponding lattice is obtained by the lattice (e_1, e_2, e_3) taking the quotient along the direction l_1 , which corresponds to e_1 . Therefore over this face the T^2 lattice is simply the plane (e_2, e_3) , and the projected vectors $-l_2$, $\frac{\partial}{\partial \phi}$, $\frac{\partial}{\partial \psi}$ are (P, Q) , (R, S) , (F, G) . The face $x = x_1$ intersects also the two faces corresponding to $\theta = 0$ and $\theta = \pi/2$, and to avoid conical singularities along the two edges where $x = x_1$ intersects these faces we must impose $hcf(R, S) = 1$ and $hcf(F, G) = 1$. Note that regularity does not require $hcf(P, Q) = 1$ since obviously the divisor $x = x_1$ does not intersect $x = x_2$.

Since R and S are coprime, it is always possible to find an $SL(2, Z)$ transformation that sends (R, S) in $(1, 0)$. With this choice the two remaining components of equation (3.2) read:

$$qQ = sG \quad (3.4)$$

$$sF - qP + r = 0 \quad (3.5)$$

We have to impose the regularity conditions at the two remaining edges of the the dual fan; by taking the appropriate quotients along the degenerating directions in the lattice (e_1, e_2, e_3) it is easy to derive the conditions $hcf(P - 1, Q) = 1$ and $hcf(F - P, G - Q) = 1$, together with the old one $hcf(F, G) = 1$. Indeed we have rederived the well known result in toric geometry that regularity is assured iff the four sides of the toric diagram $(0, 0)$, $(1, 0)$, (P, Q) , (F, G) do not pass through integers points [24].

Let's choose (p, q, r, s) coprime: we can always divide the defining equation (3.2) by a possible common factor; from $p + q = r + s$ it follows that every sub-triple of (p, q, r, s) is coprime. Then equation (3.5) says that $hcf(q, s) = 1$ otherwise a common factor should also divide r , and therefore also $p = r + s - q$. But if q and s

are coprime the general solution of (3.4) is $Q = n s$ and $G = n q$ with n an arbitrary integer $n \in \mathbb{Z}$.

Let us concentrate on the “minimal” regular case $n = 1$: $Q = s$, $G = q$. The regularity condition $hcf(F, G) = 1$ is satisfied iff $hcf(q, r) = 1$: suppose that there is an integer k that divides q and r ; then by (3.5) it divides also the product sF , but since it cannot divide s , it must divide F . So k would divide F and $G = q$. The converse is also true. Analogously it is straightforward to show, using (3.5), that the other regularity conditions are satisfied iff $hcf(p, r) = 1$ and $hcf(p, s) = 1$.

We have to determine the two remaining parameters F and P in order to complete the description of the toric diagram. Equation (3.5) has infinite solutions. In fact it is a well known result in linear Diophantine equations that when $hcf(q, s) = 1$ equation (3.5) always admits solutions, with the most general of the form:

$$\begin{cases} F = F_0 + \lambda q \\ P = P_0 + \lambda s \end{cases} \quad \lambda \in \mathbb{Z} \quad (3.6)$$

where F_0 and P_0 are particular solutions. There is not an explicit formula for F_0 and P_0 in terms of q, r, s , but of course there is an algorithm to determine the solution given the inputs q, r, s . The important point is that all the solutions (3.6) describe the same toric geometry, since there is an $SL(2, \mathbb{Z})$ transformation that sends a given solution $(0, 0)$, $(1, 0)$, (P_0, s) , (F_0, q) into any other of the family:

$$\begin{pmatrix} 1 & \lambda \\ 0 & 1 \end{pmatrix} \begin{pmatrix} P_0 \\ s \end{pmatrix} = \begin{pmatrix} P_0 + \lambda s \\ s \end{pmatrix}, \quad \begin{pmatrix} 1 & \lambda \\ 0 & 1 \end{pmatrix} \begin{pmatrix} F_0 \\ q \end{pmatrix} = \begin{pmatrix} F_0 + \lambda q \\ q \end{pmatrix} \quad (3.7)$$

To summarize, all the smooth $L^{p,q;r}$ are characterized by four coprime positive integers (p, q, r, s) such that $p + q = r + s$ and $hcf(p, r) = hcf(p, s) = hcf(q, r) = hcf(q, s) = 1$; remember also from the previous Section that a positive definite and well defined metric requires $q \geq p$. For this reason, in the following we will also denote these spaces with $L^{p,q;r,s}$. Under these conditions we can define periodicities to get a smooth CY cone with the “minimal” choice $n = 1$; the toric diagram is given by the points

$$(0, 0), \quad (1, 0), \quad (P, s), \quad (F, q) \quad (3.8)$$

where F and P correspond to any solution of (3.5). In Figure 1 we present the case $L^{p,q;r,s} = L^{1,5;2,4}$ with $F = -3$ and $P = -2$.

Notice that in the case $r = s = \bar{p}$, when one gets the known case $Y^{\bar{p},\bar{q}}$, (3.5) has always the solution $P = 0$, $F = -1$, and the toric diagram $(0, 0)$, $(1, 0)$, $(0, \bar{p})$, $(-1, \bar{p} + \bar{q})$, after a translation of $(-1, 0)$ and the $SL(2, \mathbb{Z})$ transformation $((-1, 0), (-\bar{p}, -1))$, can always be reduced to the standard form: $(0, 0)$, $(1, 0)$, $(2, \bar{p} - \bar{q})$, $(1, \bar{p})$.

We have made arbitrary choices in the previous analysis: for example one could have set the vectors corresponding to $\frac{\partial}{\partial \phi}$ and $-l_2$ equal to $(0, 0)$ and $(1, 0)$ respectively, obtaining the result in Figure 2. Again in the Figure we present the case $L^{1,5;2,4}$; obviously the toric diagram is equivalent to the previous one.

There are other non “minimal” smooth CY cones over the spaces $L^{p,q;r,s}$, that correspond to $|n| > 1$. Notice that all these smooth cases can be obtained by the “minimal” ones by multiplying the ordinates of the vertices of the toric diagram by a

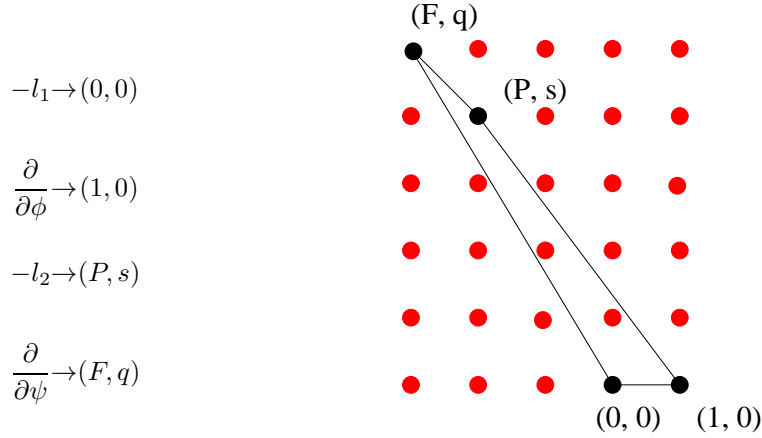


Figure 1: The toric diagram for $L^{p,q,r}$. F is typically negative and it will be renamed $-k$ in the following. The toric diagram is given by the points $(0,0), (1,0), (P,s), (-k,q)$. The explicit example in the Figure is $L^{1,5;2,4}$.

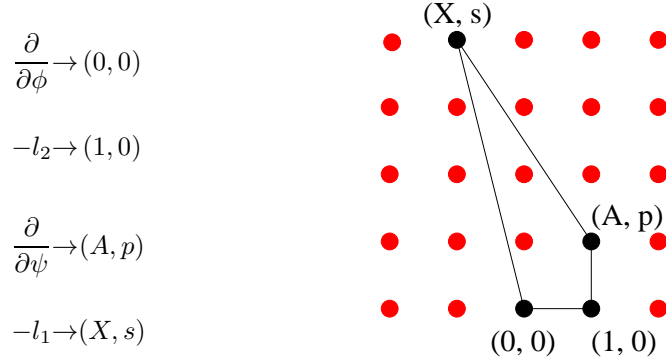


Figure 2: An alternative description for the toric diagram of $L^{p,q,r}$. The explicit example is still $L^{1,5;2,4}$. A and X satisfy the linear Diophantine equation $sA - pX - q = 0$

factor n : $q \rightarrow nq, s \rightarrow ns$. But now the request that the couples of integers p, q and r, s are pairwise coprime is no more sufficient to get a smooth manifold for a fixed n : one should check that the sides of the toric diagram do not pass through integers points. For example multiplying by $|n| > 1$ the toric diagram in Figure 2 one never gets a smooth manifold. Instead if we multiply the diagram in Figure 1 by $n \equiv 1$ or $n \equiv 2 \pmod{3}$ we find a smooth manifold (but not if n is divisible by 3). Notice also that starting from $SL(3, \mathbb{Z})$ equivalent toric diagram and multiplying by n one can get inequivalent diagrams, as in our example (see also equation (3.7)). These non “minimal” cones are Z_n quotients of the “minimal” ones. We can also abandon the request that p, q, r, s are coprime and rescale them by n in the case of Z_n quotients, so that we can continue to use the equations $G = q$ and $Q = s$ in any case. This will be understood in the following.

To finish this discussion, we notice that in describing the gauge theory we can always choose $r \leq s$, at least in smooth cases. If not so, we can exchange r with s : this does not change the geometry and therefore does not change the gauge theory. In

fact it is easy to check that the toric diagrams for $L^{p,q;r,s}$ and $L^{p,q;s,r}$ are the same up to an $SL(3, \mathbb{Z})$ transformation: start with the points $(0, 0)$, $(1, 0)$, (P, s) , (F, q) with P and F satisfying $r + F s - P q = 0$. Then apply the transformation: $((\bar{F}, x), (q, -F))$ where we can choose the integers \bar{F} and x to be solutions of $F\bar{F} + qx = 1$ (note in fact that $hcf(F, q) = 1$ in smooth cases). The resulting toric diagram is $(0, 0)$, $(1, 0)$, (\bar{P}, r) , (\bar{F}, q) with \bar{P} and \bar{F} satisfying: $s + \bar{F} r - \bar{P} q = 0$. We have therefore exchanged the role of r and s .

Analogously, when $r \leq s$, it is easy to show that it is possible to exchange the pair (p, q) with the pair (r, s) : we have to add $(-1, 0)$ to the points of the toric diagram $(0, 0)$, $(1, 0)$, (\tilde{P}, q) , (\tilde{F}, s) and then apply the transformation $((-1, \lambda), (0, 1))$. One gets the diagram: $(0, 0)$, $(1, 0)$, (\tilde{P}, q) , (\tilde{F}, s) , where now \tilde{F} and \tilde{P} satisfy the relation: $p + \tilde{F} q - \tilde{P} s = 0$, thus exchanging the role of (p, q) and (r, s) . Note that we have used transformations with determinant -1 ; moreover we expect the changes of coordinates realizing these symmetries to be non trivial.

In conclusion we can choose $p \leq r \leq s \leq q$ without loss of generality. This ordering will always be understood in the following.

3.2 Volumes from toric geometry

Recall that the Sasaki-Einstein metrics are associated with a specific vector field, the Reeb vector. Using the local form of the metric (2.2), it can be identified with $\frac{\partial}{\partial \tau}$. In [16] it was discussed a minimization procedure for determining the Reeb vector from the toric data. Recalling that, in the dual gauge theory, the Reeb vector is associated with the R-symmetry, the method discovered in [16] can be considered as the geometric dual of the a-maximization [9]. Using this algorithm one is able to compute the Reeb vector and the volume of a Sasaki-Einstein metric on the base of a toric CY cone using only the data of the toric diagram, without knowing the explicit form of the metric.

We can expand the Reeb vector of a Sasakian manifold in the basis of vectors e_i that generate the T^3 effective action

$$K = \sum_{i=1}^3 b_i e_i \quad (3.9)$$

Since in [16] it was shown that we can always set $b_1 = 3$, we can regard K as the vector $b = (3, w, t) \in \mathbb{R}^3$. We also need the vectors v^a that define the toric fan (or equivalently the inward normals to the faces of the polyhedral cone \mathcal{C}). The vectors v_a and b give enough information to find the volume of $L^{p,q,r}$ spaces [16]:

$$\text{vol}_{L^{p,q,r}} = \frac{\pi^3}{3} \sum_a \frac{(v_{a-1}, v_a, v_{a+1})}{(b, v_{a-1}, v_a)(b, v_a, v_{a+1})} \quad (3.10)$$

and the volumes of the base manifolds Σ_a (at $r = 1$) of the four special divisors

associated to the four vectors of the fan²:

$$\text{vol}_{\Sigma_a} = 2\pi^2 \frac{(v_{a-1}, v_a, v_{a+1})}{(b, v_{a-1}, v_a)(b, v_a, v_{a+1})} \quad (3.11)$$

where v_1, \dots, v_d are ordered in such way that the corresponding facets are adjacent to each other, with $v_{d+1} \equiv v_1$.

The important result of [16] is that one can find the value of b by extremizing the volume function:

$$Z_{L^{p,q,r}}(b) = \frac{1}{48\pi^3} \text{vol}_{L^{p,q,r}}(b) \quad (3.12)$$

It is possible to show that there is always only one critical point of $Z(b)$ in the dual cone \mathcal{C}^* .

We can write the function $Z(b)$ in the case of the $L^{p,q,r}$ spaces. The four vectors v^a for the case of $L^{p,q,r}$ have been determined in the previous subsection:

$$v_1 = (1, 0, 0), \quad v_2 = (1, 1, 0), \quad v_3 = (1, P, s), \quad v_4 = (1, -k, q) \quad (3.13)$$

where k and P are determined by the Diophantine equation

$$ks + qP = r \quad (3.14)$$

For a better comparison with the gauge theory Section we have renamed $F = -k$. With these values we obtain

$$Z_{L^{p,q,r}}(b) = -\frac{P^2 q^2 t + Pq(3qs - qt + 2kst) + s(k^2 st + k(3qs - 2qt + st) + q(-q + s)w)}{48t((-1 + P)t - s(-3 + w))(kt + qw)(P(-3q + t) + k(-3s + t) + (q - s)w)} \quad (3.15)$$

The minimization of this function gives algebraic equations for the determination of w and t . We were not able to solve analytically these equations. However it is easy to build a program in Mathematica for computing numerically the value of b and, consequently, the volume of the manifolds and of the special divisors for all values of p, q, r . This is the method we have used to compare the results of the volumes with the results we will obtain on the quantum field theory side.

However, we can also write explicit simple expressions for the volume of the divisors by recalling that we have a different analytic expression for the Reeb vector. The latter is indeed given by $K = \frac{\partial}{\partial \tau}$. We already provided the expression of e_i in function of $\frac{\partial}{\partial \phi}$, $\frac{\partial}{\partial \psi}$ and $\frac{\partial}{\partial \tau}$. From equation (3.9) and the results of the previous Sections we obtain

$$b = \left(3, \frac{kb_1 - a_1}{c_1}, -\frac{b_1 q}{c_1}\right) \quad (3.16)$$

It is easy to check numerically that this value indeed minimize the function $Z(b)$. With the explicit form for b we can obtain the expression of the volumes of Σ_a as functions of p, q, r ³:

$$\text{vol}_{\Sigma_{(\theta=0, r=1)}} = \frac{2\pi^2 s}{t(3s - t + Pt - sw)} = \frac{2c_1^2 \pi^2 s}{b_1 q (s + b_1 p)}$$

² (x, y, z) is the determinant of the 3×3 matrix whose rows are x, y and z respectively.

³Remember that as explained in Section 2, a_1, b_1, c_1 are known as functions of p, q, r .

$$\begin{aligned}
\text{vol}_{\Sigma_{(\theta=\pi/2, r=1)}} &= \frac{2\pi^2 r}{(kt + qw)(3r + w(s - q) - t(k + P))} \\
&= \frac{2c_1^2 \pi^2 r}{a_1 q(r + a_1 p)} \\
\text{vol}_{\Sigma_{(x=x_1, r=1)}} &= \frac{2\pi^2 q}{t(kt + qw)} = \frac{2c_1^2 \pi^2}{qa_1 b_1} \\
\text{vol}_{\Sigma_{(x=x_2, r=1)}} &= \frac{2\pi^2 p}{(s(3 - w) + t(P - 1))(3r + w(s - q) - t(P + k))} \\
&= \frac{2c_1^2 \pi^2 p}{(r + a_1 p)(s + b_1 p)} \tag{3.17}
\end{aligned}$$

One can also find the total volume of the $L^{p,q,r}$ in function of only p, q, r from the relation [16]:

$$\text{vol}_{L^{p,q,r}} = \frac{\pi}{6} \sum_a \text{vol}_{\Sigma_a} \tag{3.18}$$

4 Engineering the gauge theory

In this Section we present a constructive way for associating a gauge theory with the toric diagram of $L^{p,q,r}$. A crucial ingredient in the identification of the gauge theory is the remarkable correspondence between brane tilings and toric singularities discovered in [12]. It is based on a correspondence between dimer models and toric geometry [25].

As explained in [12], there is an elegant way to enclose all the information needed to construct the gauge theory in a single diagram, called the periodic quiver diagram. Indeed for a gauge theory living on branes placed at the tip of toric CY cone, one can extend the quiver diagram, drawing it on a torus T^2 . We associate with a gauge theory a dimer model which is simply the dual of the periodic quiver and so is still defined on a torus T^2 [12]; it has also a physical interpretation in terms of tilings of $D5$ and $NS5$ branes. An example of dimer lattice is presented in Figure 3. Nodes are colored in black and white and links connect only vertices of different color. In the brane tiling, gauge groups are represented by the faces of the dimer, the edges correspond to bifundamental matter between two gauge groups, and each term in the superpotential corresponds to a vertex [12].

The relation between dimers and toric geometry has been introduced in [25] and passes through the Kasteleyn matrix, a kind of weighted adjacency matrix of the dimer. We will explain the construction of the Kasteleyn matrix in the specific example of the $L^{p,q,r}$ singularities, even though the algorithm is completely general for dimers diagrams [12]. The matrix allows to associate a toric diagram with each dimer model, and therefore with each gauge theory. The difficult part of the game is, given the toric singularity, to determine the brane tiling that is associated with it. We have determined the tiling by analogy with the $Y^{\bar{p},\bar{q}}$ case. In this Section we present the result in an operative form; more details are given in the Appendix.

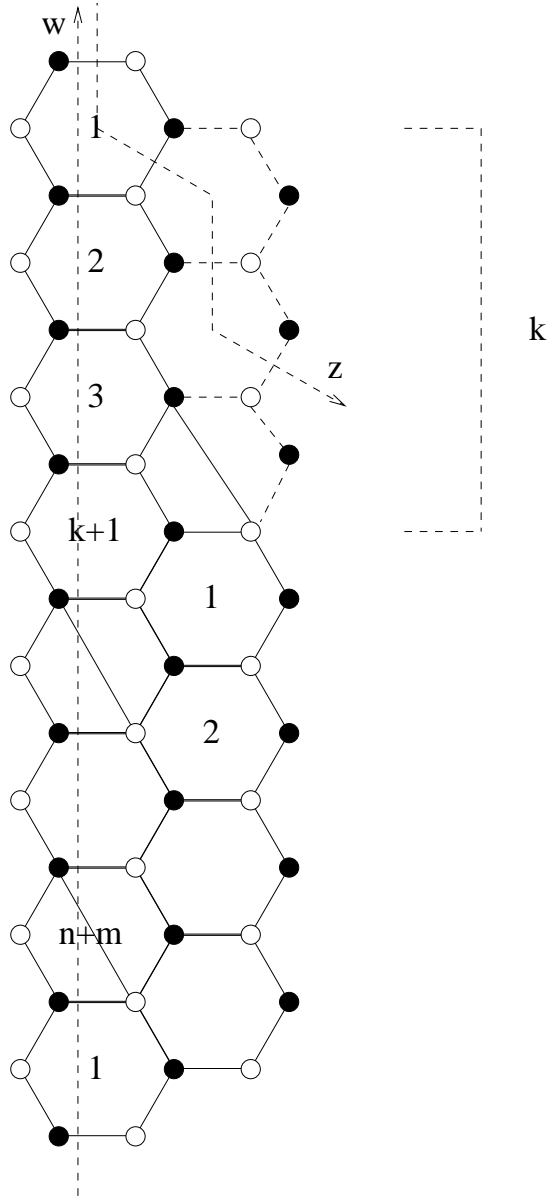
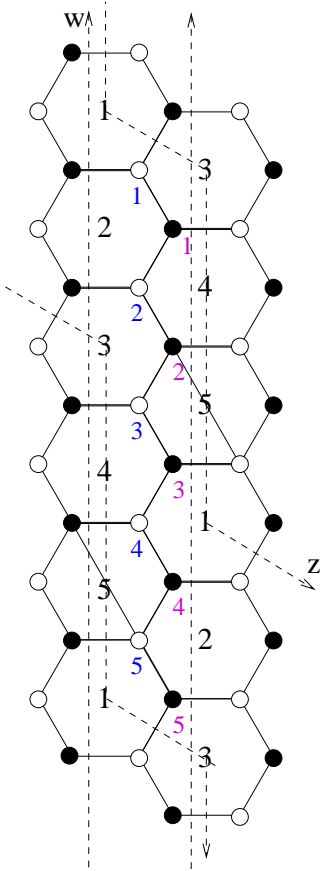


Figure 3: The brane tiling corresponding to $L^{p,q;r,s}$. The fundamental cell is composed by $n + m$ hexagons, m of which are divided in two quadrilaterals. Each face (hexagon or quadrilateral) is a gauge group, each link a bi-fundamental field and each vertex is a term in the superpotential given by the product of all the fields associated with links meeting at the vertex.

We construct now a tiling sufficiently general to contain all the smooth $L^{p,q,r}$ cases, as well as many other non-smooth cases. We can take a (dimer) lattice with a fundamental cell consisting of n hexagonal polygons and $2m$ quadrilaterals. It is convenient to picture the fundamental cell as a sequence of $n + m$ hexagons where m of them have been divided in two quadrilaterals as shown in Figure 3. The tiling is then obtained by covering the whole plane with the fundamental cell repeated infinite times. Hexagons are identified in vertical with period $n + m$. The horizontal



$$K = \begin{pmatrix} & 1 & 2 & 3 & 4 & 5 \\ 1 & 1 & 0 & 0 & w & z \\ 2 & 1 & 1 & 0 & 0 & w \\ 3 & wz^{-1} & 1 & 1 & 0 & 0 \\ 4 & 0 & wz^{-1} & 1 & 1 & 0 \\ 5 & 0 & -wz^{-1} & wz^{-1} & 1 & 1 \end{pmatrix}$$

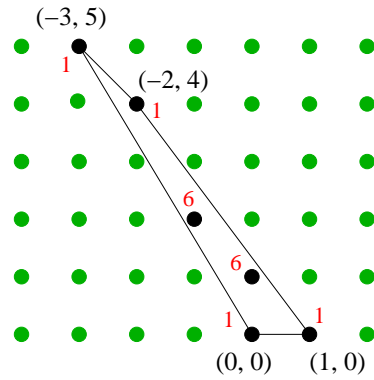


Figure 5: The toric diagram for $L^{1,5;2,4}$.

Figure 4: The dimer for $L^{1,5;2,4}$. In this case $n = 4$, $m = 1$ and $k = 3$.

identification is more complicated: each hexagon is identified with the hexagon in the column on the right which is shifted down by k positions, as indicated in Figure 3. Now we can construct the Kasteleyn matrix K . The rows are indexed by the $n + m$ white vertices and the columns are labeled by the $n + m$ black vertices. We have to draw two closed primitive cycles γ_z and γ_w on the dimer; we have chosen the cycles indicated with the dashed lines labeled with "z" and "w" in Figure 3. Then for every link in the dimer we have to add a weight in the corresponding position of K . The weight is equal to one if the link does not intersect the cycles γ_z and γ_w , and it is equal to z or $1/z$ if it intersects the cycle γ_z according to the orientation (we choose z if the white node of the link is on the right of the oriented cycle), and analogously for the γ_w cycle. We have also to multiply all the weights for diagonal links dividing the m cut hexagons by -1 : this choice fits with the request that the product of link's signs is 1 for hexagons and -1 for quadrilaterals [12]. The explicit example for $L^{1,5;2,4}$ is shown in Figures 4 and 5. With an appropriate ordering of the nodes, the $n + m$ by $n + m$ Kasteleyn matrix has a simple general form:

- Put 1 on the diagonal.

- Put 1 in the line below the diagonal and z in the position $(1, n + m)$.
- Put w in the diagonal line that is shifted by k position above the diagonal (beginning at $(1, k + 1)$); whenever w is shifted beyond the last column, it reappears in the equivalent column mod $n + m$ in the form wz^{-1} .
- Add a factor of $-w$ in the diagonal line that is shifted by $k - 1$ positions above the diagonal in all the rows labeled with the same number of a divided hexagon; whenever in this process the column is shifted beyond the last one, the factor reappears as $-wz^{-1}$ on the left.

The determinant of the Kasteleyn matrix is a Laurent polynomial $P(z, w) = \det K$ called the characteristic polynomial of the dimer model. Different choices of closed primitive cycles γ_z and γ_w multiply the characteristic polynomial by an overall power $z^i w^j$. In [12] it was conjectured that the Newton polygon of P is the toric diagram of the dual geometry. Recall that the Newton polygon of P is a convex polygon in the plane \mathbb{Z}^2 generated by the set of integer exponents of monomials in $P(z, w)$.

We have to reproduce the toric diagram of $L^{p,q;r,s}$. As we saw in the previous Section, the toric diagram of $L^{p,q;r,s}$ with $q \geq p$ is given by the convex polygon with vertices

$$[0, 0], \quad [1, 0], \quad [P, s], \quad [F, q] \quad (4.1)$$

where F and P are determined by the Diophantine equation

$$-Fs + qP = r \quad (4.2)$$

As explained in Section 3, we can also assume $p \leq r \leq s \leq q$ without any loss of generality. It is not difficult to see that the toric diagram derived from the Kasteleyn matrix in the case of the proposed tiling has vertices $(0, 0)$, $(1, 0)$, $(?, ?)$, $(-k, n + m)$. The fourth vertex can be easily determined case by case using Mathematica. We now propose the following correspondence between smooth $L^{p,q;r}$ and tiling; we have checked it up to reasonable values of $p + q$:

- For all p, q, r, s with $p \leq r \leq s \leq q$ associated with the toric diagram (4.1) consider a tiling with $n + m \equiv q$ hexagons of which $m \equiv p$ have been divided. The shift is identified with $k = -F$. The number P is associated with the positions of the divided hexagons. In the class of tiling defined by the numbers n, m, k , and distinguished by the position of the divided hexagons, there is always at least one corresponding to the diagram (4.1). It is not difficult to build an algorithm in Mathematica to check case by case that the proposed dimer theory correctly reproduces the geometry of $L^{p,q;r,s}$.

The correspondence between p, q, r, s and n, m, k is not injective nor surjective. Many tilings with the same values of n, m, k but with different order for the divided hexagons correspond to the same singularity: this is reflected in the fact that the corresponding gauge theories are connected by Seiberg dualities. Many other tilings correspond to singular horizons, having toric diagrams with integer points lying on the external sides. The zoo of cones with additional singularities is quite

vast: there are orbifolds (three edges), singular models with four sides ($L^{1,2;1,2}$ is the suspended pinch point ⁴) and so on. There are also possibly pathological models with multiplicity greater than one on the vertices of the polygon. For smooth $L^{p,q;r,s}$ we can always find a triple (n, m, k) corresponding to its toric diagram. For small values of $p + q$ ($p + q \leq 20$) and for all pairs (p, q) consisting of coprime numbers, we can always put all divided hexagons consecutively, let us say from position $n + 1$ to position $n + m$. The first non-trivial example of two different singularities associated with the same numbers n, m, k appears for $p + q = 20$: $(4, 16; 5, 15)$ and $(4, 16; 9, 11)$ both correspond to $n = 12, m = 4, k = 11$. The first can be realized with consecutive divided hexagons, the second one with divided hexagons, let us say, in positions $(1, 2, 3, 8)$. Of course, many other choice of positions for the divided hexagons are equivalent to the given ones.

Note that the Diophantine equation determine k up to integer multiple of $q = m + n$, and this fits the fact that k has a period of $n + m$ cells. Remember also that these formulae are valid for $p \leq r \leq s \leq q$. In other cases, as already explained, one can exchange r with s and the pair (p, q) with (r, s) .

5 The gauge theory

In this Section we present the conformal gauge theories associated with the manifolds $L^{p,q;r,s}$, we compute the central charge and the dimensions of the fields and we compare with the geometrical results obtained in Section 3.

As we saw in the previous Section, the dimer model (n, m, k) that corresponds to the gauge theory dual to smooth $L^{p,q;r,s}$ is given by a tiling like that in Figure 3 with numbers:

$$\begin{cases} n = q - p \\ m = p \end{cases} \quad (5.1)$$

$$r - k s - P q = 0$$

There is always a choice of positions for the m divided hexagons corresponding to this singularity. As discussed previously, in many simple cases the hexagons can be disposed consecutively, let us say from the $n + 1$ to the $n + m$ position.

As in previous Sections, we consider, without loss of generality, $p \leq r \leq s \leq q$.

The gauge theory on the worldvolume of N D3-branes living at the toric singularity is then constructed with the following rules. The brane tiling gives an Hanany-Witten construction of the gauge theory using D5 and NS5 branes [12]. The faces in the brane tiling represent a finitely extended D5 brane and the edges represent NS branes bounding the D5 branes. The configuration is roughly obtained from the original D3 branes by applying two T-dualities which convert D3 branes in D5 branes and encode in the NS branes the geometrical information about the singularity. Starting with N D3 branes, we obtain N D5 branes covering the torus. Each face is then associated with a $U(N)$ gauge group. Each edge between adjacent faces gives rise to a chiral field transforming in the bi-fundamental representation of the corresponding gauge

⁴The class of models with additional singularities $L^{p,q;p,q}$ has been studied in detail in [21].

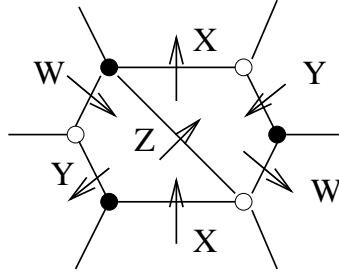


Figure 6: The arrows indicate the chirality of the bi-fundamental fields associated with the edges in the brane tiling.

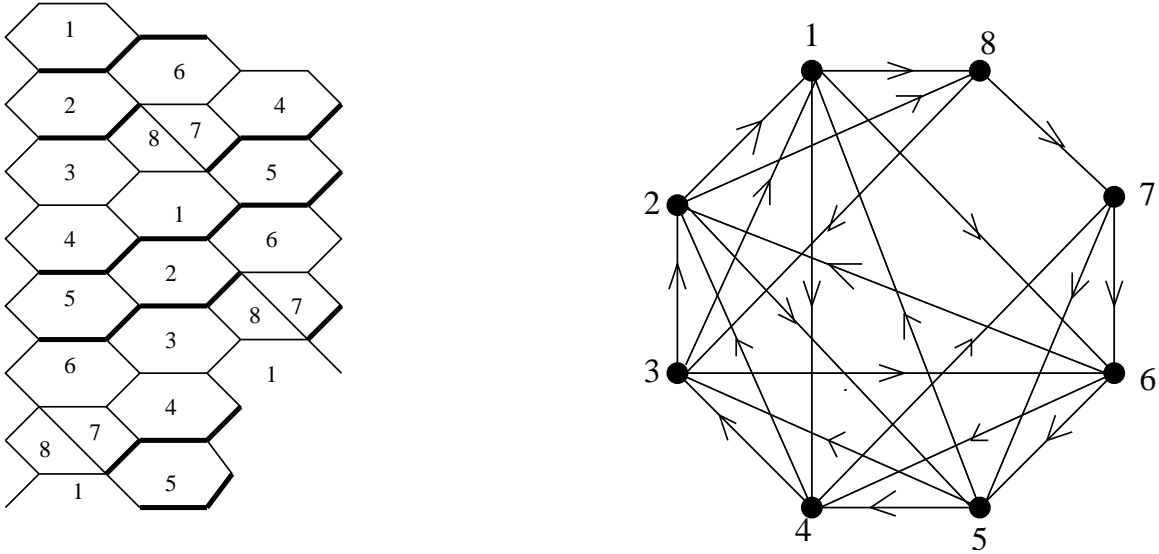


Figure 7: The brane tiling for $L^{1,7;3,5}$ and the more conventional quiver diagram (where nodes are gauge groups and oriented links chiral bi-fundamentals). The bold edges indicate, among the X and W fields, those called \tilde{X} and \tilde{W} , with different R charge. In this case, $n = 6$, $m = 1$ and $k = 2$.

groups. The chirality of the matter fields is determined by the natural orientation of the edges induced by the dimer lattice. For practical purposes, the orientation of the fields is indicated with arrows in Figure 6. Fields associated with horizontal edges are conventionally named X , those associated with diagonal edges are named Y and W depending on the slope of the edge and, finally, a special name Z is reserved to fields connecting quadrilaterals. Each vertex in the tiling corresponds to a superpotential term in the gauge theory obtained by multiplying the fields associated with the edges that meet in the given vertex. The total number of gauge group is $n_{\text{groups}} = p + q$, the number of fields is $n_{\text{fields}} = 3q + p$ and the number of superpotential terms is $n_{\text{pot}} = 2q$. We obviously have ⁵

$$n_{\text{groups}} - n_{\text{fields}} + n_{\text{pot}} = 0 \quad (5.2)$$

With this simple set of rules we can associate a gauge theory with each tiling. The

⁵This relation is a consequence of the topology of the lattice [12], as discussed in the Appendix.

case of $L^{1,7;3,5}$ is pictured in Figure 7 with the more familiar quiver description aside.

The AdS/CFT correspondence predicts that the gauge theory dual to $AdS_5 \times L^{p,q;r,s}$ is superconformal. We can prove that the theory described in the previous paragraph flows in the infrared to a superconformal fixed point with standard methods [26]. Conformal invariance requires two sets of conditions. The first one is that the beta function of all the gauge groups vanishes. We know that, for a supersymmetric gauge theory, the beta function is proportional to [27]

$$3T(\text{adj}) - \sum_i T(r_i)(1 - 2\gamma_i) \quad (5.3)$$

where γ_i is the anomalous dimension of the i -th chiral multiplet transforming in the r_i representation of the gauge group. $T(r_i)$ is the Casimir of the r_i representation normalized such that $T(\text{adj}) = N$ and $T(\text{fundamental}) = 1/2$. Recall now that, at a superconformal fixed point, dimension and R-charge of a chiral field are related by $R_i = 2\Delta_i/3 = 2(1 + \gamma_i)/3$. In our case, where all the fields are bi-fundamentals, the vanishing of the beta functions gives a set of $p + q$ equations,

$$\beta_k = 2 + \sum_{i_k} (R_{i_k} - 1) = 0 \quad (5.4)$$

where the sum is extended only to the fields charged under the k -th group. Conditions (5.4) can be re-interpreted as the requirement that the R-symmetry is anomalous free ⁶. This is not a mysterious result. As is well known, in a superconformal theory, the trace of the stress-energy tensor and the $U(1)_R$ anomaly belong to the same supermultiplet. As a consequence, the vanishing of the beta function gives the same condition as the cancellation of the anomaly.

The second sets of conditions come from the requirement that each term in the superpotential has dimension three, which means R-charge 2. We have a total of $2q$ such conditions. We see from relation (5.2) that the number of constraints imposed by conformal invariance is equal to the number of unknown R-charges. However, not all the conditions are linearly independent. It is not difficult to see that, for integers p, q, r, s corresponding to smooth metrics $L^{p,q;r,s}$, there are exactly three redundant conditions. This means that all the R-charges can be expressed in terms of three unknown variables. The reason why we found a three parameter solution of the set of conditions for conformal invariance is that, given a non-anomalous R-symmetry, we can obtain another one by adding all non-anomalous global $U(1)$ symmetries. In our specific case, we can see that there are exactly three non-anomalous global $U(1)$ symmetries from the number of massless vectors in the AdS dual. Since the manifold is toric, the metric has three $U(1)$ isometries. One of these (the Reeb one) corresponds to the R-symmetry while the other two are related to non-anomalous global $U(1)$ s. A third gauge field in AdS comes from the reduction of the RR four form on the non-trivial S^3 in $L^{p,q;r,s}$; in the supergravity literature the corresponding vector multiplet is known as the Betti multiplet.

⁶Recall that the charge of the fermion in the chiral multiplet is $R - 1$. The charge of a gaugino is conventionally normalized to 1.

The existence of a three parameter solution of the conditions for conformal invariance is enough to establish the existence of a fixed point. The gauge theory indeed depends on n_{group} gauge couplings and n_{pot} superpotential couplings. Conformal invariance only impose $n_{\text{group}} + n_{\text{pot}} - 3$ conditions on these couplings, generically leaving a three-dimensional complex space of solutions corresponding to a three dimensional manifold of conformal field theories.

We can go further and solve explicitly the conditions for conformal invariance in terms of three unknown R-charges, x, y, z . In this process, we discover that many fields have the same R-charge. Some examples are reported in the Appendix. We can extrapolate from the results and give a general recipe: we find that, in all cases, there are

- p Z fields with charge z
- r X fields with charge x
- q Y fields with charge y
- $q - r$ X fields with charge $x + z$; they will be called \tilde{X} from now on, to distinguish them from the other X fields.
- $q - s$ W fields with charge $2 - y - x$
- s W fields with charge $2 - x - y - z$; they will be called \tilde{W} from now on, to distinguish them from the other W fields.

The distinction among the X and W fields is not easy to formalize. We will try to do that by explaining the following graphical rule:

- Start at the bottom-right vertex of one divided hexagon. Call \tilde{W} the W field attached to this vertex. Always by moving down in the vertical direction make the following steps. Move down by k hexagons. If you are at the bottom-right vertex of a regular hexagon, call \tilde{X} and \tilde{W} the X and W fields meeting at this vertex and then move down by $k + 1$ steps; instead if you are at the bottom-right vertex of a divided hexagon call \tilde{W} the W field attached to this vertex and move down by k steps. Repeat the procedure until you go back to the starting point. All the fields you have encountered in this way define the set of \tilde{X} and \tilde{W} fields. In Figure 3 these fields are marked in bold.

Note that in order to reproduce the correct counting of the different kinds of fields, during the “cycle” described in the algorithm above, one has to touch all the m cut hexagons and $q - r$ of the normal hexagons. In this way one gets $q - r$ fields of \tilde{X} -type and $q - r + p = s$ fields of \tilde{W} -type. The existence of a single “cycle” with such features is also the requirement that allows to find a correct distribution of cuts among the $n + m$ hexagons for a given $L^{p,q;r,s}$ theory. Further details are given in the Appendix.

One can check that this procedure works exactly in the case where p, q, r, s define smooth manifolds. It is not difficult to verify that for $r = s = \bar{p}, p = \bar{p} - \bar{q}, q = \bar{p} + \bar{q}$ we recover the quiver gauge theory for $Y^{\bar{p},\bar{q}}$ determined in [5]. The Y and Z fields

correspond to the fields denoted with the same name in [5]. The \tilde{W} and X fields are now degenerate, in the sense that they connect the same pair of gauge groups, and corresponds to the U_α doublets in [5]. Finally the \tilde{X} and W fields are degenerate and correspond to the V_α doublets.

At the fixed point, only one of the possible non-anomalous R-symmetries enters in the superconformal algebra. It is the one in the same multiplet as the stress-energy tensor. The actual value of the R-charges at the fixed point can be found by using the a-maximization technique [9]. As shown in [9], we have to maximize the a-charge [28]

$$a(R) = \frac{3}{32}(3\text{Tr}R^3 - \text{Tr}R) \quad (5.5)$$

If we sum the conditions (5.4) for all gauge groups, we discover that

$$0 = p + q + \sum_i (R_i - 1) = \text{Tr}R \quad (5.6)$$

so that we can equivalently maximize $\text{Tr}R^3$.

In our case,

$$a = \frac{9}{32}(p + q + s(1 - x - y - z)^3 + (q - s)(1 - y - x)^3 + q(y - 1)^3 + r(x - 1)^3 + (q - r)(x + z - 1)^3 + p(z - 1)^3) \quad (5.7)$$

The results of the maximization give a complete information about the values of the central charge and the dimensions of chiral operators at the conformal fixed point. These can be compared with the prediction of the AdS/CFT correspondence [29,30]. The first important point is that the central charge is related to the volume of the internal manifold [29]

$$a = \frac{\pi^3}{4\text{Vol}(L^{p,q;r,s})} \quad (5.8)$$

Moreover, recall that in the AdS/CFT correspondence a special role is played by baryons. The gravity dual describes a theory with $SU(N)$ gauge groups, in our case $\prod_i^{p+q} SU(N)$. The fact that the groups are $SU(N)$ and not $U(N)$ allows the existence of dibaryons. Each bi-fundamental field Φ_α^β gives rise to a gauge invariant baryonic operator

$$\epsilon^{\alpha_1 \dots \alpha_N} \Phi_{\alpha_1}^{\beta_1} \dots \Phi_{\alpha_N}^{\beta_N} \epsilon_{\beta_1 \dots \beta_N}$$

There is exactly one non-anomalous baryonic symmetry. It is sometime convenient to think about it as a non-anomalous combination of $U(1)$ factors in the enlarged $\prod_i^{p+q} U(N)$ theory. In the AdS dual the baryonic symmetry corresponds to the Betti multiplet (the reduction of the RR four-form) and the dibaryons are described by a D3-brane wrapped on a non-trivial three cycle. The R-charge of the i -th field can be computed in terms of the volume of the corresponding cycle Σ_i using the formula [30]

$$R_i = \frac{\pi \text{Vol}(\Sigma_i)}{3\text{Vol}(L^{p,q;r,s})} \quad (5.9)$$

All the volumes appearing in these formulae can be extracted from Section 3 and compared with the result of the a-maximization. Although we cannot analytically solve the maximization equations for all p, q, r, s , it is not difficult to compare the results of the two Sections using Mathematica. Both the geometrical computation using toric geometry and the a-maximization involve solving algebraic equations, and this can be easily automatized. Several detailed examples of the comparison are presented in the Appendix. The agreement of the two methods is absolutely remarkable.

In Table 1 we present the charges of the chiral fields. We also included the assignment of charges under the baryonic $U(1)_B$ symmetry since it plays a special role among the global symmetries. The $U(1)_B$ can be identified using the following AdS-inspired arguments. All fields should have non zero charge since they all define corresponding dibaryons, described in the gravitational dual as D3 branes charged under the RR four-form. Moreover, the cubic anomaly for $U(1)_B$ should vanish since no Chern-Simons term in the five dimensional supergravity can contain three vector fields coming from reduction of the RR four-form [5]. A little patience shows that the assignments in the Table are the ones that satisfy these conditions.

	Z	X	Y	\tilde{X}	W	\tilde{W}
$U(1)_R$	z	x	y	$x+z$	$2-y-x$	$2-x-y-z$
$U(1)_B$	q	$-s$	p	$q-s$	$s-p$	$-r$

Table 1: charges under the R-symmetry and the baryonic symmetry.

6 Adding fractional branes

In this Section we discuss the inclusion of fractional branes, the duality cascade and the infrared physics of the non-conformal theories.

Since the topology of smooth $L^{p,q;r,s}$ is $S^3 \times S^2$ we expect the existence of a single type of fractional brane we can add in order to obtain non-conformal theories. The fractional brane is a D5 wrapped on the S^2 which is vanishing at the tip of the cone. The addition of M fractional branes gives a theory with the same number of gauge groups, but with different number of colors

$$\prod_i^{p+q} SU(N_i) \tag{6.1}$$

and the same bi-fundamental fields as before. The numbers N_i correspond to the unique assignment of gauge groups that lead to a non anomalous theory. These numbers can be easily determined from the baryonic symmetry: the difference between the number of colors of gauge groups connected by a bi-fundamental is M times the baryonic charge of the chiral field, with the convention that fields of opposite chirality contribute with opposite sign. As a practical recipe, one can start with

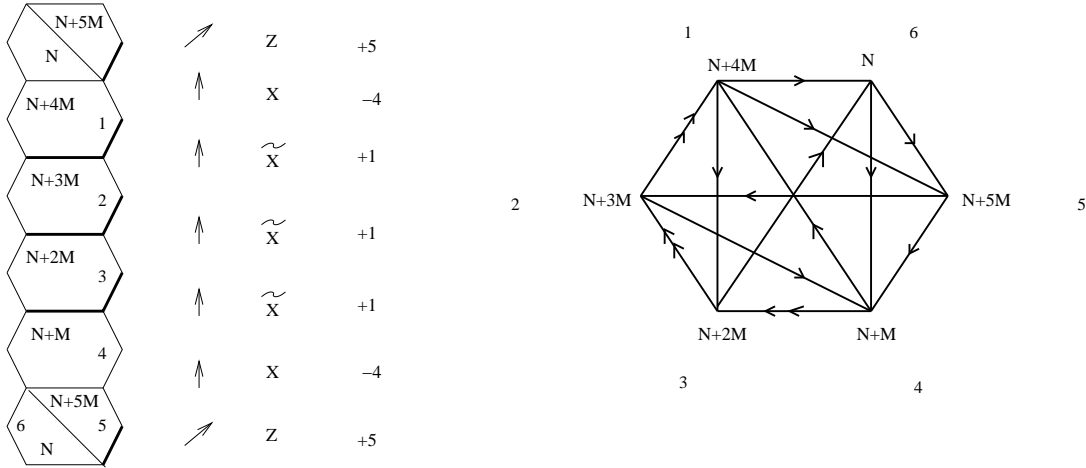


Figure 8: The quiver for N physical and M fractional branes in $L^{1,5;2,4}$. The number of colors are determined using the baryonic symmetry. Double arrows indicate that two different bi-fundamental fields are connecting two nodes.

a face in the tiling (or a node in the dual quiver), assign to it a conventional number of colors N , find the numbers in the adjacent faces using the previous rule and then continue until all numbers N_i are determined. As an example, the case of $L^{1,5;2,4}$ is pictured in Figure 8. The method works for the following reasons [19, 31]. First of all, the cancellation of all anomalies for the baryonic symmetry implies that the sum of charges for all the bi-fundamental fields starting from a given face must vanish

$$\text{face } k : \quad \sum_{i_k} q_{i_k} = 0 \quad (6.2)$$

This condition ensures that, with the previous assignment, all gauge groups are not anomalous. In addition, the fact that the baryonic symmetry is a combination of the $U(1)$ factors in $\prod_i^{p+q} U(N_i)$ guarantees that the result is independent of the choice of path on the tiling used for determining the N_i s.

The theories with fractional branes undergoes repeated Seiberg dualities thus giving rise to cascades. This phenomenon is familiar for the conifold [3] and has been studied for many other quiver theories associated with toric singularities [32], including the $Y^{\bar{p},\bar{q}}$ case [7]. One can easily verify that cascades exist also for $L^{p,q;r,s}$. For simplicity, we consider the case of $L^{1,5;2,4}$. As indicated in Figure 8, the gauge theory is

$$\prod_{k=0}^5 SU(N + kM) \quad (6.3)$$

A Seiberg duality on the gauge group with the largest number of colors leads to a theory of the same form with $N \rightarrow N - M$. Perhaps, the simplest way to check this is to use the graphical method discussed in [12] (see Figure 9).

From the point of view of the AdS/CFT correspondence, we could expect to find a supergravity solution describing the cascade along the lines of the Klebanov-Strassler

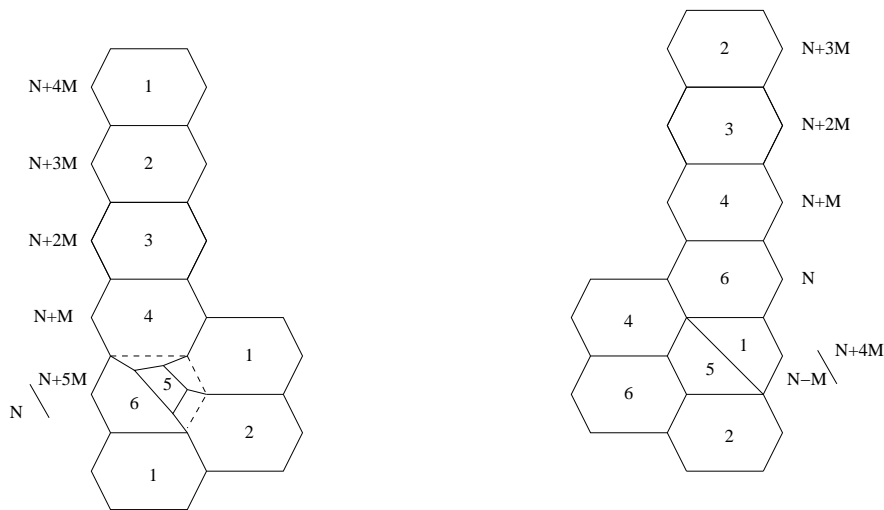


Figure 9: Duality cascade for $L^{1,5;2,4}$. The fifth gauge group undergoes a Seiberg duality. This amounts to deform it as indicated in the left picture. The new vertices where only two edges meet are quadratic terms in the superpotential. The corresponding massive fields should be integrated out. Rearranging the vertices and recalling that under Seiberg duality $N_c \rightarrow N_f - N_c$ (the fifth gauge group will change number of colors from $N + 5M$ to $N - M$), we get the picture on the right. We obtain the original tiling with a relabeling of the gauge groups. The net effect on the theory is the shift $N \rightarrow N - M$. We refer to [12] for a description of Seiberg duality in the brane tiling context.

one [3]. Certainly, it is possible to construct a solution with fractional branes on the singular cone [33]. This is the analogous of the Klebanov-Tseytlin solution for the conifold [34]. This kind of background has been constructed for the $Y^{\bar{p},\bar{q}}$ case in [7]. However, it is plausible that, in most cases, there is no regular supersymmetric solution describing the infrared physics of the cascade. The counterpart of this statement in quantum field theory is the fact that all these gauge theories have no supersymmetric vacuum. Here we briefly discuss the motivation for these negative results both from the supergravity and the gauge theory side [17, 18, 20, 42].

From the point of view of supergravity, it is known that the cones over smooth $L^{p,q;r,s}$ manifolds have no complex deformations. The reason is a mathematical result [35] that states that deformations of isolated Gorenstein toric singularities are in one-to-one correspondence with decomposition of the toric diagram in Minkowski sums of polytopes⁷. In the class of toric diagram which are the convex hull of four points and corresponds to smooth horizons, only the conifold and its relatives can be decomposed. Clearly, the toric diagram in Figure 1 cannot be decomposed as sum of polytopes. This means that the cones over smooth $L^{p,q;r,s}$ have no complex deformations. The argument is not definitive. It rules out the possibility of imitating the Klebanov-Strassler solution, where the original conifold singularity has been deformed. One could argue that more general solution may exist. The Klebanov-Strassler metric has a metric that is conformally Calabi-Yau, but more general su-

⁷The Minkowski sum of a convex polygon P is a set of other convex polygons P_i such that all $t \in P$ can be written as $t = \sum t_i, t_i \in P_i$.

persymmetric solutions exist. One could for example expect a solution based on $SU(3)$ structure like that describing the baryonic branch of Klebanov-Strassler [36]. However all type IIB supersymmetric solutions with $SU(3)$ structure must have complex internal manifolds [39, 40] and the argument in [35] just forbids the existence of complex deformations of our cone. It seems that supersymmetric solutions with non complex manifolds exist in the class of $SU(2)$ structures [41]. In any case, if a solution exists it is quite non trivial.

This discussion is mirrored in quantum field theory by the fact that all these theories flow in the infrared to cases where at least one gauge group has number of flavors less than the number of colors. In this situation, we expect the generation of a non perturbative ADS superpotential that will destabilize the vacuum, like in SQCD. Let us examine the concrete case of $L^{1,5;2,4}$ for definiteness. Ignoring minor subtleties ⁸, the cascade will reach a point where $N = 0$. The gauge group is now

$$SU(M) \times SU(2M) \times SU(3M) \times SU(4M) \times SU(5M) \quad (6.4)$$

The $SU(5M)$ factor has only $4M$ flavors. We can make two kinds of $SU(5M)$ gauge invariant mesons $\mathcal{M}_{14} \sim YX$ and $\mathcal{M}_{12} \sim Y\tilde{W}$ and combine them in a square matrix $\mathcal{M} = (\mathcal{M}_{12}, \mathcal{M}_{14})$. A non perturbative $1/\det(\mathcal{M})^\alpha$ superpotential will be generated. The presence of a tree-level superpotential does not seem to help: the runaway behavior induced by the ADS superpotential wins over the stabilizing effect of the tree-level superpotential. The only other relevant terms in the superpotential are indeed linear both in \mathcal{M} and in the remaining fields leading to a superpotential that schematically reads

$$\frac{1}{\det(\mathcal{M})^\alpha} + \mathcal{M}_{12}\tilde{X} + \mathcal{M}_{14}W + \dots \quad (6.5)$$

without any other occurrence of W . There is no supersymmetric vacuum for finite values of the fields. We have not studied the general case with arbitrary p, q, r, s but we strongly expect that the situation encountered for $L^{1,5;2,4}$ is generic. In known examples (reference [19] contains the discussion of several different class of singularities), whenever the geometry forbids the existence of a deformation the gauge theory has a runaway potential.

It is interesting to observe that our discussion is valid for the case of smooth $L^{p,q;r,s}$. For particular values of (non coprime) p, q, r, s , the manifolds $L^{p,q;r,s}$ exhibit additional singularities. In some cases of diagrams with four vertices but with integer points on the sides, there are complex deformations. For example, $L^{1,2;1,2}$ is called in the literature the Suspended Pinch Point and it is known to admit a deformation. It would be interesting to understand if our improved knowledge of the metric for these singular horizons can help in constructing new regular supergravity duals of $N = 1$ supersymmetric gauge theories.

⁸At the last step of the cascade one gauge factor has the same number of colors and flavors and we should study the quantum deformed moduli space of this theory instead of naively perform a Seiberg duality [37, 38]. The result however does not change.

7 Conclusions

In this paper we presented the superconformal gauge theory dual to the type IIB background $AdS \times L^{p,q,r}$ constructed in [10,11]. The metric has only $U(1)^3$ isometry thus making difficult to determine the dual CFT using only symmetries. Fortunately, we could take advantage of an important progress recently made in the study of the correspondence between toric singularities and CFTs, the brane tiling construction [12]. This ingredient, combined with the analysis of the toric geometry of $C(L^{pqr})$, allowed us to determine the gauge theory.

The number of explicit metrics for Sasaki-Einstein horizons than can be used in the AdS/CFT correspondence is rapidly increasing. There are two aspects of the correspondence where these metrics can give interesting results, the conformal case and the non-conformal one.

On the conformal side, the most striking results come from the comparison between conformal quantities at the fixed point and volumes. The geometrical counterpart of the a-maximization [9] is the volume minimization proposed in [16] for determining the Reeb vector for toric cones. The agreement of the two types of computation suggests that some more deep connection between CFT quantities and geometry is still to be uncovered. In particular, it would be interesting to understand this agreement from the point of view of the brane tiling construction. To demystify a little bit the importance of having an explicit metric, we should note that all relevant volumes are computed for calibrated divisors. This means that these volumes can be computed from the toric diagram without actually knowing the metric. Explicit formulae are given in [16]: the volume minimization procedure only relies on the vectors defining the toric fan. Therefore, with a correspondence between toric diagram and gauge theories, as that provided by the brane tiling, many checks of the AdS/CFT correspondence can be done without an explicit knowledge of the metric.

Where the metric is really necessary is the non-conformal side. All these models typically admit fractional branes and can be used for the construction of new duals for confining $N = 1$ gauge theories. The existence of a duality cascade is a general feature and this can be used for engineering string compactifications with local throats, perhaps with multiple scales. We expect to find regular supersymmetric backgrounds whenever the singularity has a complex deformation. This is not the case for all the smooth manifolds in the class $L^{p,q,r}$, except for the trivial case corresponding to the conifold ($L^{1,1,1} = T^{1,1}$). From the quantum field theory point of view, there is indeed no supersymmetric vacuum. At the end of the cascade, a destabilizing superpotential is generated, similar to that of SQCD. The runaway potential forbids even non-supersymmetric vacua [19]. Cases of singularities which admit deformations are known, for example the delPezzo singularities [42] (with at least five edges in the toric fan). Unfortunately, the metrics for the cone in this case is unknown. It would be very interesting to see if one can find new examples of deformable horizons, for example using the metrics for (singular) $L^{p,q;p,q}$.

Acknowledgements We would like to thank Sergio Benvenuti and Alessan-

dro Tomasiello for helpful discussions. This work is supported in part by by INFN and MURST under contract 2001-025492, and by the European Commission TMR program HPRN-CT-2000-00131.

Appendix

A.1 The dimer model

In this Section, by analogy with the $Y^{\bar{p},\bar{q}}$ case, we construct the tiling configuration (dimer model) for the $L^{p,q,r}$ manifolds.

From the toric diagram that describes the geometry of the CY cone, it is possible to derive immediately some features of the gauge theory living on a stack of N D3-brane at the tip of the cone.

First of all the number of the gauge groups: as explained in the works of Hanany and collaborators, it is simply given by the double area of the toric diagram. A straightforward calculation yields: $Area = (p + q)/2$, so the number of the gauge groups is $p + q = r + s$.

The number of bifundamental chiral fields can be deduced from the (p, q) web, which is obtained simply by taking the outward pointing normals to the sides of the toric diagram. The legs of the (p, q) web are the integer vectors:

$$(0, -1) \quad (s, 1 - P) \quad (q - s, P - F) \quad (-q, F) \quad (\text{A.1})$$

and the formula for the number of fields is simply

$$n_{\text{fields}} = \frac{1}{2} \sum_{i,j} \left| \det \begin{pmatrix} p_i & q_i \\ p_j & q_j \end{pmatrix} \right| \quad (\text{A.2})$$

where i, j run over the four vectors of the (p, q) web. In our case the previous formula yields: $n_{\text{fields}} = 2(p + q) + |p - s| + |q - s|$.

To define a $\mathcal{N} = 1$ gauge theory it is not enough to give the quiver diagram, that encodes only the information about the gauge groups and the bifundamental matter. One must also write the superpotential for chiral fields. As explained in [12], there is an elegant way to enclose all the information needed to construct the gauge theory in a single diagram, called the periodic quiver diagram. Indeed for a gauge theory living on branes placed at the tip of toric CY cone, one can extend the quiver diagram, drawing it on a torus T^2 . The vertices represent still gauge groups, the oriented links are bifundamental matter as usual, and the faces of the periodic quiver correspond to superpotential terms in the gauge theory: every superpotential term is the trace of the product of chiral fields in a face of the periodic quiver. From the Euler formula for a torus

$$V - E + F = 0 \quad (\text{A.3})$$

with V =vertices=number of gauge groups, E =edges=number of fields, and F =faces=number of terms in the superpotential, one can deduce that in our case $F = p + q + |p - s| + |q - s|$.

Note that the numbers of gauge groups, superpotential terms and chiral fields just deduced are relative to a particular toric phase of the gauge theory: remember that a toric phase is characterized by a quiver where all the gauge groups have the same number of colors N , the number of D3-branes. There can be different toric phases for the same physical gauge theory, generally connected by Seiberg dualities and possibly characterized by different values for the numbers of fields and superpotential terms. We will exhibit a toric phase for the gauge theory on $L^{p,q,r}$ with content described by the numbers just derived.

To build the gauge theory from the toric data, one can apply the so called Inverse Algorithm [43], based on partial resolution of the toric singularity. Since a fast version of this algorithm is still lacking, we preferred to guess the gauge theory and then check it through the Fast Forward Algorithm [12]. In fact to check the correctness of the gauge theory one must show that its moduli space reproduces the geometry: in the case of one brane $N = 1$, it must be exactly the CY cone. In [12] it was proposed a fast algorithm to compute the moduli space of the gauge theory using dimer technology; we briefly review it here.

The dimer model of the gauge theory is simply the dual of the periodic quiver and so is still defined on a torus T^2 ; it has also a physical interpretation in terms of tilings of $D5$ and $NS5$ branes, as explained in Section 5. However we will need only the fact that now gauge groups are represented by the faces of the dimer, the edges correspond to bifundamental matter between two gauge groups, and each term in the superpotential corresponds to a vertex. Note that the superpotential is a sum of positive and negative terms, with each field appearing exactly once in a positive term and once in a negative term. This is reflected by the fact that the dimer's vertices are colored with black or white and links connect only vertices of different color.

The moduli space of supersymmetric vacua is a toric symplectic cone whose toric diagram is easily reconstructed from the dimer model. The relation between dimers and toric geometry have been introduced in [25] and passes through the Kasteleyn matrix, a kind of weighted adjacency matrix of the dimer.

We will describe the construction of the Kasteleyn matrix on the specific example of $Y^{\bar{p},\bar{q}}$, even though the algorithm is completely general for dimers diagrams [12]. The gauge theories on $Y^{\bar{p},\bar{q}}$ have dimers built only with n hexagons and $2m$ quadrilaterals, that can be obtained by dividing in two parts m hexagons drawn below the first n ones (see Figure 10). There is only one column of such hexagons and divided hexagons that are periodically identified in the vertical direction. The other T^2 periodicity is described by drawing other columns and identifying each face with the face in the right column shifted down by one position ($k = 1$).

For the case of $Y^{\bar{p},\bar{q}}$ the number n and m are given by: $n = 2\bar{q}$, $m = \bar{p} - \bar{q}$, so that we have the correct number of gauge groups: $n + 2m = 2\bar{p}$, superpotential terms: $2(n + m) = 2\bar{p} + 2\bar{q}$, and the correct number of fields: $3n + 4m = 4\bar{p} + 2\bar{q}$.

The rows in the Kasteleyn matrix K are indexed by the $n + m$ white vertices (labeled with blue numbers in figure 10) and the columns are labeled by the $n + m$ black vertices (labeled with red numbers). We have to draw two closed primitive cycles γ_z and γ_w on the dimer; we have chosen the cycles indicated with the dashed

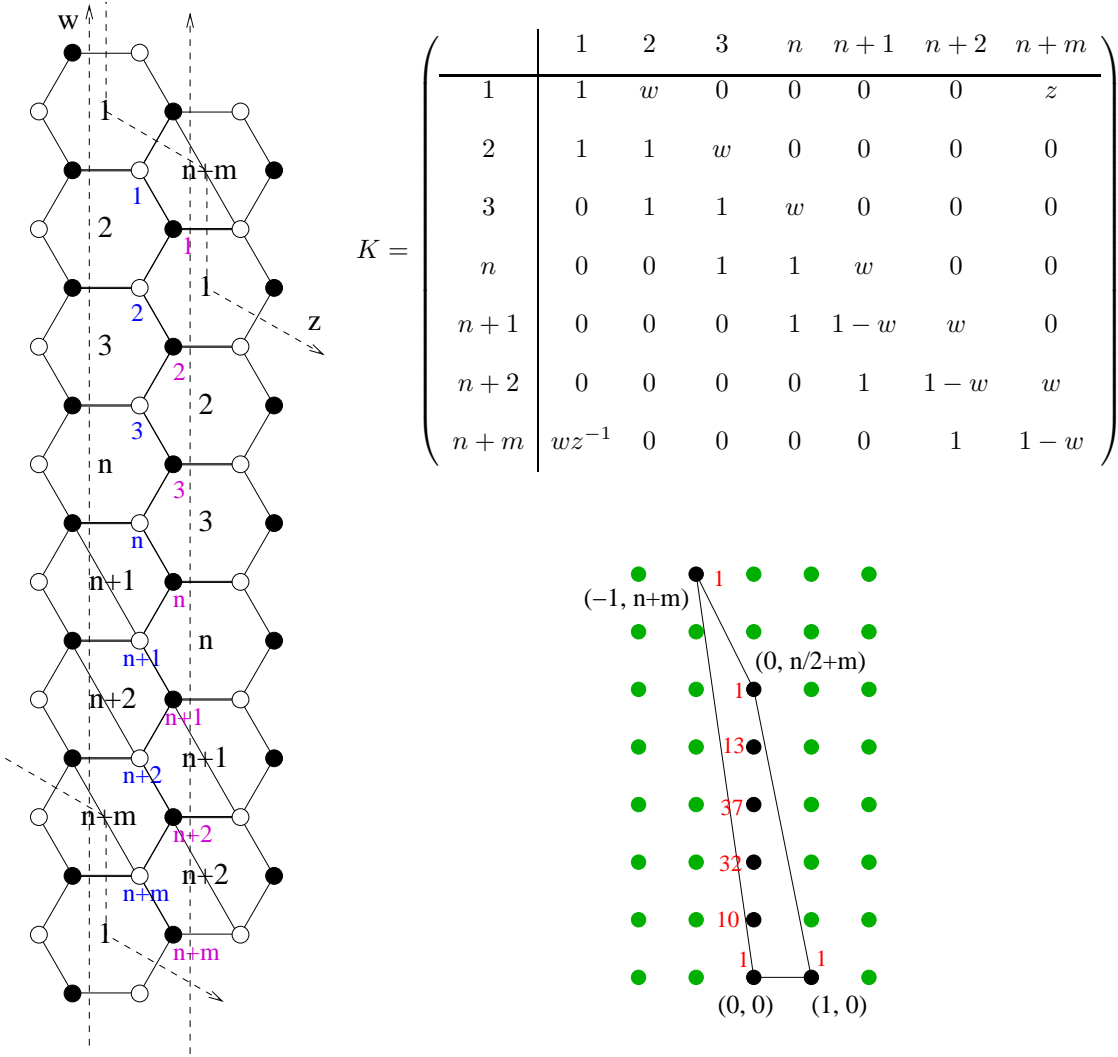


Figure 10: The dimer for $Y^{\bar{p},\bar{q}}$

Figure 11: The toric diagram for $Y^{\bar{p},\bar{q}}$. Multiplicities refer to $Y^{5,2}$.

lines labeled with "z" and "w" in Figure 10. Then for every link in the dimer we have to add a weight in the corresponding position of K . The weight is equal to one if the link does not intersect the cycles γ_z and γ_w , and it is equal to z or $1/z$ if it intersects the cycle γ_z according to the orientation (we choose z if the white node of the link is on the right of the oriented cycle), and analogously for the γ_w cycle. We have also to multiply these weight by -1 for the diagonal links dividing the last m hexagons in quadrilaterals: this choice fits with the request that the product of link's signs is 1 for hexagons and -1 for quadrilaterals.

The determinant of the Kasteleyn matrix is a Laurent polynomial $P(z, w) = \det K$ called the characteristic polynomial of the dimer model. Different choices of closed primitive cycles γ_z and γ_w multiply the characteristic polynomial by an overall power $z^i w^j$.

The Newton polygon is a convex polygon in the plane \mathbb{Z}^2 generated by the set

of integer exponents of monomials in $P(z, w)$. In [12] it was conjectured that the Newton polygon of P is the toric diagram of the geometry. This is the essential part of the Fast Forward Algorithm, since the determinant of K for a given quiver allows one to reconstruct easily the dual toric geometry. Moreover the absolute value of coefficients in $P(z, w)$ give the multiplicities of chiral fields in the Witten sigma model associated to the gauge theory.

In the case represented in Figure 10 with $n=4$, $m=3$ and $k=1$, corresponding to $Y^{5,2}$, the determinant of the Kasteleyn matrix is

$$P(z, w) = \det K = 1 - 10w + 32w^2 - 37w^3 + 13w^4 - w^5 + \frac{w^7}{z} + z \quad (\text{A.4})$$

and give the toric diagram pictured in Figure 11.

For general values of m and even n with $k = 1$ it is easy to prove that the toric diagram is given by: $(0, 0)$, $(1, 0)$, $(0, n/2 + m)$, $(-1, n + m)$, that is: $(0, 0)$, $(1, 0)$, $(0, \bar{p})$, $(-1, \bar{p} + \bar{q})$, which is the correct form given in section 3 for $Y^{\bar{p}, \bar{q}}$.

The vertex $(0, 0)$ comes from the 1 along the diagonal. The diagonal line of 1 below the diagonal together with the element z in the corner $(1, n + m)$ gives the vertex $(1, 0)$ of the toric diagram. The diagonal line of w above the diagonal, together with the element wz^{-1} in the corner $(n + m, 1)$ gives the vertex $(-1, n + m)$. The last point of the diagram is built with the maximal number of ws (and no zs) in the determinant, which is $n/2 + m$.

Now it is easy to generalize this to the case of arbitrary k . The simplest case is $k = 0$ where $P(z, w)$ can be explicitly calculated as:

$$P(z, w) = (1 + w)^{n+m} + (-1)^{n+m-1} z(1 - w)^m \quad k = 0 \quad (\text{A.5})$$

which gives the toric diagrams: $(0, 0)$, $(1, 0)$, $(1, m)$, $(0, n + m)$. Since two sides of the diagram pass through integer points, it corresponds to non smooth manifolds, $L^{p,q;p,q}$, already studied in detail in [21].

For more general values of k one gets new toric cones; in particular we looked for the values of (n, m, k) that give the gauge theory for smooth $L^{p,q,r}$ and we have verified that all these smooth cases can be realized through an appropriate choice of (n, m, k) .

First of all one has to understand the form of the Kasteleyn matrix in the general case where also k can vary. Consider, for simplicity, the case of consecutive hexagons. With our notations and conventions K is a $(n + m, n + m)$ matrix with the factors 1 and factor z placed in the same position as for $k = 1$. But now the factors w , $-w$ and wz^{-1} must be all shifted by k positions along the horizontal direction: the continuous diagonal of w and wz^{-1} begins at position $(1, k + 1)$. If a factor w (or $-w$) is shifted beyond the last column, it reappears in the equivalent column mod $(n+m)$ in the form wz^{-1} (or $-wz^{-1}$). See also the explicit example of $L^{1,5,2,4}$ that corresponds to $n = 4$, $m = 1$, $k = 3$ in figures 4 and 5.

So it is easy to see that the principal diagonal and the continuous diagonal below the principal one still give factors of 1 and z in the determinant, corresponding to the vertices $(0, 0)$ and $(1, 0)$. Moreover there's a continuous diagonal made of k factors

of wz^{-1} and $n + m - k$ factors of w corresponding to the vertex $(-k, n + m)$. The remaining vertex is harder to find; in general the toric diagram is $(0, 0), (1, 0), (?, ?), (-k, m + n)$.

Now consider the case $p \leq r \leq s \leq q$. We want to fit our counting of fields, gauge groups and superpotential terms with the counting in the dimer theory (n, m, k) . Our formulae reduce to:

$$\begin{aligned} \# \text{ gauge} &= p + q = n + 2m \\ \# \text{ super potential} &= 2q = 2(n + m) \\ \# \text{ fields} &= p + 3q = 3n + 4m \end{aligned} \tag{A.6}$$

These formulae are solved by $n = q - p$ and $m = p$. Moreover note that the toric diagram for $L^{p,q,r}$: $(0, 0), (1, 0), (P, s), (F, q)$ fits with the diagram from the dimer model since $m + n = q$ and gives the identification:

$$F = -k \tag{A.7}$$

and this directly gives the way to calculate k for $L^{p,q;r,s}$: k and P are the solution of the linear Diophantine equation: $r - k s - P q = 0$.

It is easy to generalize to the case where the divided hexagons are not in consecutive positions. The form of the Kasteleyn matrix is explained in Section 4. Tilings with divided hexagons in arbitrary positions are necessary to describe all possible $L^{p,q;r,s}$.

To summarize, the dimer model (n, m, k) that defines the gauge theory dual to the geometry of smooth $L^{p,q;r,s}$ is given by:

$$\begin{cases} n = q - p \\ m = p \end{cases} \tag{A.8}$$

$$r - k s - P q = 0$$

and has associated toric diagram given by: $(0, 0), (1, 0), (P, s), (-k, q)$. Note that the Diophantine equation determine k up to integer multiple of $q = m + n$, and this fits the fact that k is a periodicity in a dimer with $n + m$ cells (n hexagons and m hexagons divided in two quadrilaterals). In our pictures we use the solution with $0 \leq k \leq m + n$.

Remember that these formulae are valid for $p \leq r \leq s \leq q$. In other cases, as already explained, one can exchange r with s and the pair (p, q) with (r, s) .

At this point it is not difficult to build an algorithm in Mathematica to check case by case that the proposed dimer theory correctly reproduces the geometry of $L^{p,q,r}$. We have also checked that the multiplicities of external vertices in toric diagram associated to smooth $L^{p,q,r}$ are always equal to one.

A.2 Computing R charges

In this subsection we present an explicit example focusing on the problem of computing the R charges for the field theory, and in particular we explain the algorithm,

already discussed in Section 5, to distinguish between fields X , W and \tilde{X} , \tilde{W} , once a good distribution for the cuts on the hexagons has been found.

Consider to be concrete the case $(p, q; r, s) = (2, 8; 3, 7)$ that gives $(n, m, k) = (6, 2, 5)$ and $P = -4$. In this case it is possible to choose all the cut hexagons to be consecutive. We have in total $3n + 4m$ fields (=26) that we number as in Figure 12. The general rule is: start from the white bottom-right vertex of the first hexagon, and call the links attached to it (1,2,3): the first is a W -type field, the second is X -type field and the third is a Y field. Then pass to the bottom-right vertex of the second face and continue to label the triple of fields in this order until the last white vertex is reached. At the end label the remaining m Z fields. So we can arrange the $3n + 4m$ fields in an array divided in $n + m$ triples of fields (W, X, Y) (or with tilded W or X) and m fields of Z type:

$$\begin{array}{cccccccc} 1 & | & 2 & | & 3 & | & 4 & | & 5 & | & 6 & || & 7 & | & 8 & || \\ \text{fields} = & (1, 2, 3|4, 5, 6|7, 8, 9|10, 11, 12|13, 14, 15|16, 17, 18||19, 20, 21|22, 23, 24||25, 26) \end{array}$$

where the numbers in the upper line label the $n + m$ triples. Correspondingly we have an array R of $3n + 4m$ R -charges organized as in the previous formula.

We have to find all the possible assignments of R charges that make the theory conformal. The condition of zero β function for every gauge group explained in Section 5 becomes:

$$\sum_{i_k \in \text{hex}} R_{i_k} = 4 \quad \sum_{i_k \in \text{quad}} R_{i_k} = 2 \quad (\text{A.9})$$

that is the sum of R charges of the edges of every hexagon must be equal to 4 and must be equal to 2 for quadrilaterals. Then we have to impose that every term in the superpotential has R charge equal to 2; this is a condition for links attached to the same vertex:

$$\sum_{i_h \in \text{vertex}} R_{i_h} = 2. \quad (\text{A.10})$$

This set of $3n + 4m$ linear conditions can be organized in a matricial form: $C_{ij}R_j = V_i$, where each line i is an equation that must be imposed. C_{ij} is a $(3n + 4m, 3n + 4m)$ matrix, R_j is the array of $3n + 4m$ R charges and V_i is the vector of non homogeneous known terms (made up only with 4 and 2).

To write the most general solution for R_j we have to know a particular solution v^0 and the ker of the matrix C_{ij} . Then the array R can be written as

$$R = v^0 + z v^1 + y v^2 + x v^3 \quad (\text{A.11})$$

where v^0 is a particular solution and v^1 , v^2 and v^3 are in the ker of C :

$$C_{ij}v_j^0 = V_i, \quad C_{ij}v_j^k = 0, \quad k = 1, 2, 3. \quad (\text{A.12})$$

and x , y and z are arbitrary real variables.

In fact we know on physical grounds that in cases corresponding to gauge theories dual to $L^{p,q;r,s}$ the dimension of the ker of C_{ij} is exactly 3: the vectors v^1 , v^2 and v^3 are a basis of non anomalous $U(1)$ global symmetries and we know that $L^{p,q;r,s}$ has two flavor $U(1)$ and one baryonic $U(1)$. Indeed it is easy to write an algorithm to build the matrix C_{ij} and check this statement in all the desired cases.

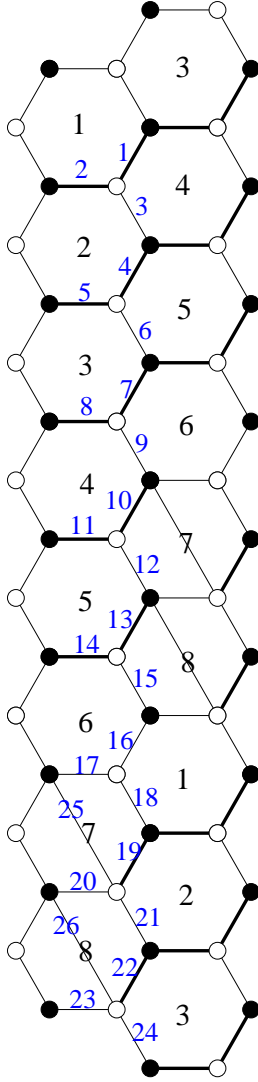


Figure 12: The dimer for $L^{2,8;3,7}$

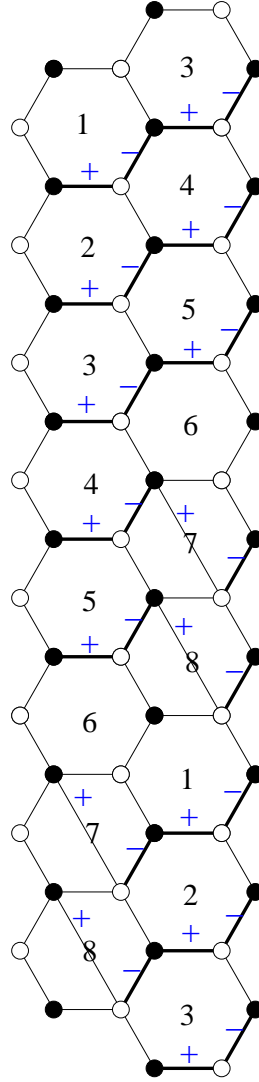


Figure 13: The charge v^1 for $L^{2,8;3,7}$

The form of v^0 and of two of the vectors in the kernel of C_{ij} is easy to find:

$$\begin{array}{l}
 \begin{array}{cccccccc}
 1 & | & 2 & | & 3 & | & 4 & | & 5 & | & 6 & || & 7 & | & 8 & || \\
 v^0 = & (2,0,0 & | & 2,0,0 & | & 2,0,0 & | & 2,0,0 & | & 2,0,0 & | & 2,0,0 & || & 2,0,0 & | & 2,0,0 & || & 0,0) \\
 v^2 = & (-1,0,1 & | & -1,0,1 & | & -1,0,1 & | & -1,0,1 & | & -1,0,1 & | & -1,0,1 & || & -1,0,1 & | & -1,0,1 & || & 0,0) \\
 v^3 = & (-1,1,0 & | & -1,1,0 & | & -1,1,0 & | & -1,1,0 & | & -1,1,0 & | & -1,1,0 & || & -1,1,0 & | & -1,1,0 & || & 0,0)
 \end{array}
 \end{array}$$

and this is true for generic values of (n, m, k) : it is easy to show that a particular solution v^0 of the equations (A.9) and (A.10) can be obtained by assigning R charge equal to 2 to all W and \tilde{W} and zero to all the other fields.

Analogously one can get two vectors in the ker of C_{ij} by assigning charge -1 to W and \tilde{W} , 1 to the fields Y , and zero to all other fields (this is the vector v^2) or by assigning charge -1 to W and \tilde{W} , charge 1 to X and \tilde{X} and zero to the other fields.

It is easy to check for these assignments that the sum of charges in every vertex is zero (the superpotential is conserved by the $U(1)$ symmetry) and the sum of charges for every face is zero (cancellation of the anomaly for the $U(1)$ symmetry), thus v^2 and v^3 are in $\ker C$.

The remaining $U(1)$ symmetry v^1 is more tricky to find; we want to show that it can be built by giving charge 1 to all Z fields, charges $(-1, 0, 0)$ to the m triples corresponding to the cut hexagons, and charges $(-1, 1, 0)$ or $(0, 0, 0)$ to the triples corresponding to normal hexagons (in this way charge cancellation is automatically satisfied for white vertices). Then proceed as in Figure 13: consider one of the divided hexagons, for instance the last (8). We have to impose charge conservation on the black top left vertex; so we must assign charge $(-1, 1, 0)$ to the triple corresponding to face number 5. Now looking at the black bottom left vertex of face 5 we see that we have to put another $(-1, 1, 0)$ to the triple corresponding to face 3. Repeating this operation we find the cycle:

$$8 \xrightarrow{+k} 5 \xrightarrow{+k+1} 3 \xrightarrow{+k+1} 1 \xrightarrow{+k+1} 7 \xrightarrow{+k} 4 \xrightarrow{+k+1} 2 \xrightarrow{+k+1} 8$$

where we have to add k if we are in a cell with a cut or $k + 1$ if we are in a normal hexagon (modulo $(n + m)$). We assign $(-1, 1, 0)$ to all the triples corresponding to normal hexagons touched by the cycle and $(0, 0, 0)$ to the remaining ones. In our concrete example we find:

$$\begin{array}{cccccccc} 1 & | & 2 & | & 3 & | & 4 & | & 5 & | & 6 & || & 7 & | & 8 & || \\ v^1 = & (-1, 1, 0) & | & (-1, 1, 0) & | & (-1, 1, 0) & | & (-1, 1, 0) & | & (-1, 1, 0) & | & (0, 0, 0) & | & (-1, 0, 0) & | & (-1, 0, 0) & | & (1, 1) \end{array}$$

All the cut hexagons are covered by this cycle; their corresponding charges are $(-1, 0, 0)$. The fact that the cycle closes assures that charge is conserved also at all black vertices. Then it is easy to see that this algorithm also assures that the sum of charges for every face is zero (anomaly cancellation).

This algorithm allows to find the right disposition of fields once the distribution of cuts on the hexagons has been found. It corresponds to the algorithm on the dimer to distinguish between fields X , \tilde{X} and W , \tilde{W} given in Section 5. It also allows to count the number of different kinds of fields: if the cycle closes after touching all the m cut hexagons and N normal hexagons, we must have:

$$m k + N (k + 1) = \lambda(m + n) \tag{A.13}$$

for some integer λ . This is equivalent to the equation:

$$(k + 1) (m + n - N) + (m + n) (\lambda - 1) = k (n + 2 m) \tag{A.14}$$

Now consider the problem of finding $(p, q; r, s)$ given (n, m, k) : rewriting the equation $r - k s - P q = 0$ we find that:

$$(k + 1) r - (m + n) P = k (n + 2 m) \tag{A.15}$$

This problem has not a unique solution for r and P , even requiring $p \leq r \leq s \leq q$. In fact $hcf(m + n, k + 1)$ is not necessarily equal to 1. So we see that it is possible to get the same values of (n, m, k) for different theories $(p, q; r, s)$.

When the problem (A.15) has a unique solution, in the cases $hcf(m+n, k+1) = 1$ (which is always true if p and q are coprime), we see by comparing expressions (A.14) and (A.15) that $m+n-N = r$: they are solution of the same Diophantine equation with $0 \leq (m+n-N), r \leq (m+n)$.

Using $N = m+n-r = q-r$ and equation (A.11) we again find that there are: p fields of Z type, r X , q Y , $(q-r)$ \tilde{X} , $(q-s)$ W and s \tilde{W} . This counting must be true also in the general case since it always gives the right expression for the central charge a and for the R charges of chiral fields that match the predictions of the AdS/CFT correspondence.

We conclude that the requirement for finding a good distribution of cuts for a theory dual to smooth $L^{p,q;r,s}$ is the existence of a unique “cycle”, built with the algorithm described above, touching all the m cut hexagons and $N = q-r$ of the normal hexagons. This “cycle” must be unique since there are only three $U(1)$ charges.

A.3 Some examples

In table 2 we report the results of numerical analysis for $L^{p,q;r,s}$ with number of gauge groups $p+q \leq 16$. We list all the smooth “minimal” (in the sense that they are not orbifolds) cases that do not belong to the already known family $Y^{\tilde{p},\tilde{q}}$. We give for every $(p, q; r, s)$ the values of (n, m, k) and of the quantity P entering in the toric diagram ($0 \leq k \leq q-1$), the total volume, the central charge a and the R charges $R(Y) = y$, $R(\tilde{W})$, $R(Z) = z$, $R(X) = x$, (the remaining charges can be computed through the expressions in function of x, y, z given in the text).

The important point to note is that the same numbers can be obtained from the formulae in Section 2 and 3. In particular, the volume, computed through equation (2.19) or by the method described subsection (3.2) following [16], always matches the value for a computed using the standard AdS/CFT formula. This matching is true also for the volumes of the divisors, computed as in subsection (3.2), and the values of R charges of the fields Y , \tilde{W} , Z , and X , computed through a maximization. In fact we find:

$$R(Y) = \frac{\pi \text{vol}(\Sigma_{x=x_1})}{3 \text{vol}} \quad R(\tilde{W}) = \frac{\pi \text{vol}(\Sigma_{\theta=0})}{3 \text{vol}}$$

$$R(Z) = \frac{\pi \text{vol}(\Sigma_{x=x_2})}{3 \text{vol}} \quad R(X) = \frac{\pi \text{vol}(\Sigma_{\theta=\pi/2})}{3 \text{vol}}$$

The relation between the total volume and a was recently demonstrated in algebraic way by [21], and the comparison between the geometrical formulae for volumes of divisors and R-charges was done in [22].

We also checked in these cases that the dimer configuration always reproduces the geometry by computing the Kasteleyn matrix. In these cases it is possible to put all the cuts in the $n+m$ hexagons in consecutive positions, and we believe that this is true every time there is only one choice of $(p, q; r, s)$ with $p \leq r \leq s \leq q$, at least for smooth cases. This happens for example if $hcf(n+m, k+1) = 1$, that is for p and q coprime.

But as discussed few lines above the map from $(p, q; r, s)$ to (n, m, k) is in general not injective; the smallest example of a pair of values of $(p, q; r, s)$ (smooth and “minimal” case) that give the same (n, m, k) is obtained for 20 gauge groups: one can check that $(p, q; r, s) = (4, 16; 5, 15)$ and $(p, q; r, s) = (4, 16; 9, 11)$ using the formulas in this article give both $(n, m, k) = (12, 4, 11)$. These two theories are not equivalent, but they can both be obtained with $(n, m, k) = (12, 4, 11)$ with appropriate choices for disposition of the cuts among the $12+4=16$ hexagons. By computation of the Kasteleyn matrix, one can see that the “standard” choice with all consecutive cuts corresponds to $(p, q; r, s) = (4, 16; 5, 15)$. The other theory $(4, 16; 9, 11)$ can be obtained putting the cuts in the positions $(1, 2, 3, 8)$ where $1, 2, \dots, 16$ label the $n + m$ hexagons (but there are obviously many equivalent choices obtained for example performing Seiberg dualities). We have checked that this also happens in many other cases.

We believe that all smooth $L^{p,q;r,s}$ can be obtained by an opportune choice of m cuts in the tiling with $n + m$ hexagons and shift k where (n, m, k) are obtained through the formulas in this article (probably this is not the only way to represent the gauge theory associated to $L^{p,q;r,s}$, but hopefully this choice can be used as a canonical representation). It would therefore be interesting to understand better this point and maybe write an algorithm that allows one to find the distribution of cuts in the tiling.

(p,q,r,s)	(n,m,k)	P	Vol	a	R(Y)	R(W)	R(Z)	R(X)
(1,5,2,4)	(4,1,3)	-2	5.7248	1.35403	0.632216	0.593238	0.286325	0.48822
(1,7,2,6)	(6,1,5)	-4	4.196	1.84737	0.643002	0.617373	0.265531	0.474093
(1,7,3,5)	(6,1,2)	-1	4.22672	1.83394	0.644448	0.594397	0.229036	0.532119
(1,9,2,8)	(8,1,7)	-6	3.30707	2.34394	0.64869	0.629624	0.254868	0.466819
(2,8,3,7)	(6,2,5)	-4	3.46292	2.23845	0.622014	0.596865	0.329893	0.451228
(1,11,2,10)	(10,1,9)	-8	2.72765	2.84185	0.652184	0.637012	0.248404	0.4624
(1,11,3,9)	(10,1,4)	-3	2.74414	2.82477	0.653604	0.625732	0.202214	0.518451
(1,11,4,8)	(10,1,6)	-4	2.75273	2.81596	0.654573	0.615195	0.17831	0.551922
(1,11,5,7)	(10,1,7)	-4	2.757	2.81159	0.655113	0.604008	0.166451	0.574428
(2,10,3,9)	(8,2,7)	-6	2.8393	2.7301	0.631576	0.612381	0.31603	0.440013
(3,9,4,8)	(6,3,5)	-4	2.936	2.64018	0.606051	0.582591	0.363364	0.447995
(3,9,5,7)	(6,3,2)	-1	2.95615	2.62218	0.605623	0.55581	0.347596	0.490971
(4,8,5,7)	(4,4,3)	-2	3.01039	2.57494	0.574958	0.545937	0.408526	0.470578
(1,13,2,12)	(12,1,11)	-10	2.32051	3.34045	0.654545	0.641948	0.244071	0.459436
(1,13,3,11)	(12,1,5)	-4	2.33298	3.32261	0.65585	0.633048	0.195902	0.515201
(1,13,4,10)	(12,1,3)	-2	2.33981	3.3129	0.656791	0.625167	0.169647	0.548394
(1,13,5,9)	(12,1,2)	-1	2.3437	3.30741	0.657396	0.617305	0.154768	0.570531
(1,13,6,8)	(12,1,4)	-2	2.34573	3.30455	0.657732	0.608744	0.147015	0.586509
(3,11,4,10)	(8,3,7)	-6	2.4791	3.12677	0.617705	0.59939	0.348088	0.434817
(1,15,2,14)	(14,1,13)	-12	2.01893	3.83945	0.656246	0.645477	0.240967	0.45731
(2,14,3,13)	(12,2,11)	-10	2.08323	3.72094	0.642184	0.629183	0.300885	0.427748
(2,14,5,11)	(12,2,3)	-2	2.10746	3.67816	0.643822	0.60599	0.243022	0.507166
(3,13,5,11)	(10,3,4)	-3	2.15875	3.59077	0.625837	0.595104	0.313746	0.465313
(4,12,5,11)	(8,4,7)	-6	2.19639	3.52923	0.606287	0.588973	0.369229	0.435511
(5,11,7,9)	(6,5,2)	-1	2.25203	3.44204	0.582711	0.53978	0.392348	0.485161

Table 2: central charges and R-charges for $L^{p,q;r,s}$

References

- [1] I. R. Klebanov and E. Witten, Nucl. Phys. B **536**, 199 (1998) [arXiv:hep-th/9807080].
- [2] B. S. Acharya, J. M. Figueroa-O'Farrill, C. M. Hull and B. Spence, Adv. Theor. Math. Phys. **2**, 1249 (1999) [arXiv:hep-th/9808014]; D. R. Morrison and M. R. Plesser, Adv. Theor. Math. Phys. **3**, 1 (1999) [arXiv:hep-th/9810201].
- [3] I. R. Klebanov and M. J. Strassler, JHEP **0008**, 052 (2000) [arXiv:hep-th/0007191].
- [4] J. P. Gauntlett, D. Martelli, J. Sparks and D. Waldram, Class. Quant. Grav. **21**, 4335 (2004) [arXiv:hep-th/0402153]; "Sasaki-Einstein metrics on $S(2) \times S(3)$," arXiv:hep-th/0403002; "A new infinite class of Sasaki-Einstein manifolds," arXiv:hep-th/0403038.
- [5] S. Benvenuti, S. Franco, A. Hanany, D. Martelli and J. Sparks, "An infinite family of superconformal quiver gauge theories with Sasaki-Einstein duals," arXiv:hep-th/0411264.
- [6] M. Bertolini, F. Bigazzi and A. L. Cotrone, JHEP **0412**, 024 (2004) [arXiv:hep-th/0411249].
- [7] Q. J. Ejaz, C. P. Herzog and I. R. Klebanov, "Cascading RG Flows from New Sasaki-Einstein Manifolds," arXiv:hep-th/0412193.
- [8] S. Benvenuti and M. Kruczenski, "Semiclassical strings in Sasaki-Einstein manifolds and long operators in $N = 1$ gauge theories," arXiv:hep-th/0505046.
- [9] K. Intriligator and B. Wecht, Nucl. Phys. B **667**, 183 (2003) [arXiv:hep-th/0304128].
- [10] M. Cvetič, H. Lu, D. N. Page and C. N. Pope, "New Einstein-Sasaki spaces in five and higher dimensions," arXiv:hep-th/0504225.
- [11] D. Martelli and J. Sparks, "Toric Sasaki-Einstein metrics on $S^{**2} \times S^{**3}$," arXiv:hep-th/0505027.
- [12] A. Hanany and K. D. Kennaway, "Dimer models and toric diagrams," arXiv:hep-th/0503149; S. Franco, A. Hanany, K. D. Kennaway, D. Vegh and B. Wecht, "Brane dimers and quiver gauge theories," arXiv:hep-th/0504110.
- [13] A. Hanany and A. Zaffaroni, JHEP **9805**, 001 (1998) [arXiv:hep-th/9801134].
- [14] A. Hanany and A. M. Uranga, JHEP **9805**, 013 (1998) [arXiv:hep-th/9805139].
- [15] A. Hanany and E. Witten, Nucl. Phys. B **492**, 152 (1997) [arXiv:hep-th/9611230].
- [16] D. Martelli, J. Sparks and S. T. Yau, "The Geometric Dual of a-maximization for Toric Sasaki-Einstein Manifolds," arXiv:hep-th/0503183.

- [17] A. Butti and A. Zaffaroni, unpublished.
- [18] D. Berenstein, C. P. Herzog, P. Ouyang and S. Pinansky, “Supersymmetry Breaking from a Calabi-Yau Singularity,” arXiv:hep-th/0505029.
- [19] S. Franco, A. Hanany, F. Saad and A. M. Uranga, “Fractional branes and dynamical supersymmetry breaking,” arXiv:hep-th/0505040.
- [20] M. Bertolini, F. Bigazzi and A. L. Cotrone, “Supersymmetry breaking at the end of a cascade of Seiberg dualities,” arXiv:hep-th/0505055.
- [21] S. Benvenuti and M. Kruczenski, “From Sasaki-Einstein spaces to quivers via BPS geodesics: Lpqr,” arXiv:hep-th/0505206.
- [22] S. Franco, A. Hanany, D. Martelli, J. Sparks, D. Vegh and B. Wecht, “Gauge theories from toric geometry and brane tilings,” arXiv:hep-th/0505211.
- [23] D. Martelli and J. Sparks, “Toric geometry, Sasaki-Einstein manifolds and a new infinite class of AdS/CFT duals,” arXiv:hep-th/0411238.
- [24] Fulton, “Introduction to Toric Varieties”, Princeton University Press.
- [25] A. Okounkov, N. Reshetikhin and C. Vafa, “Quantum Calabi-Yau and classical crystals,” arXiv:hep-th/0309208; R. Kenyon, A. Okounkov and S. Sheffield, “Dimers and Amoebae,” arXiv:math-ph/0311005.
- [26] R. G. Leigh and M. J. Strassler, Nucl. Phys. B **447**, 95 (1995) [arXiv:hep-th/9503121].
- [27] V. A. Novikov, M. A. Shifman, A. I. Vainshtein, M. B. Voloshin and V. I. Zakharov, Nucl. Phys. B **229**, 394 (1983); V. A. Novikov, M. A. Shifman, A. I. Vainshtein and V. I. Zakharov, Nucl. Phys. B **229**, 381 (1983); Phys. Lett. B **166**, 329 (1986).
- [28] D. Anselmi, D. Z. Freedman, M. T. Grisaru and A. A. Johansen, Nucl. Phys. B **526**, 543 (1998) [arXiv:hep-th/9708042]; D. Anselmi, J. Erlich, D. Z. Freedman and A. A. Johansen, Phys. Rev. D **57**, 7570 (1998) [arXiv:hep-th/9711035].
- [29] S. S. Gubser, Phys. Rev. D **59**, 025006 (1999) [hep-th/9807164].
- [30] S. S. Gubser and I. R. Klebanov, Phys. Rev. D **58**, 125025 (1998) [arXiv:hep-th/9808075].
- [31] S. Benvenuti, A. Hanany and P. Kazakopoulos, “The toric phases of the $Y(p,q)$ quivers,” arXiv:hep-th/0412279.
- [32] B. Feng, A. Hanany and Y. H. He, JHEP **0108**, 040 (2001) [arXiv:hep-th/0104259]; S. Franco, A. Hanany, Y. H. He and P. Kazakopoulos, “Duality walls, duality trees and fractional branes,” arXiv:hep-th/0306092; S. Franco, Y. H. He, C. Herzog and J. Walcher, Phys. Rev. D **70**, 046006 (2004) [arXiv:hep-th/0402120].

- [33] D. Gepner and S. S. Pal, “Branes in $L(p,q,r)$,” arXiv:hep-th/0505039.
- [34] I. R. Klebanov and A. A. Tseytlin, Nucl. Phys. B **578**, 123 (2000) [arXiv:hep-th/0002159].
- [35] K. Altmann, “The versal Deformation of an isolated toric Gorenstein Singularity”, alg-geom/9403004.
- [36] A. Butti, M. Grana, R. Minasian, M. Petrini and A. Zaffaroni, JHEP **0503**, 069 (2005) [arXiv:hep-th/0412187].
- [37] O. Aharony, JHEP **0103** (2001) 012 [arXiv:hep-th/0101013].
- [38] S. S. Gubser, C. P. Herzog and I. R. Klebanov, JHEP **0409**, 036 (2004) [arXiv:hep-th/0405282].
- [39] A. R. Frey, “Notes on $SU(3)$ structures in type IIB supergravity,” JHEP **0406**, 027 (2004) [arXiv:hep-th/0404107].
- [40] M. Graña, R. Minasian, M. Petrini and A. Tomasiello, “Supersymmetric backgrounds from generalized Calabi-Yau manifolds,” JHEP **0408**, 046 (2004) [arXiv:hep-th/0406137].
- [41] G. Dall’Agata, “On supersymmetric solutions of type IIB supergravity with general fluxes,” Nucl. Phys. B **695**, 243 (2004) [arXiv:hep-th/0403220].
- [42] S. Franco, A. Hanany and A. M. Uranga, “Multi-flux warped throats and cascading gauge theories,” arXiv:hep-th/0502113.
- [43] B. Feng, A. Hanany and Y. H. He, Nucl. Phys. B **595**, 165 (2001) [arXiv:hep-th/0003085].